IDEA League

Master of Science in Applied Geophysics

Research Thesis

Seismic Deblending By Shot Repetition

Sixue Wu

August 8, 2014

Seismic Deblending By Shot Repetition

Master of Science Thesis

for the degree of Master of Science in Applied Geophysics at
Delft University of Technology
ETH Zürich
RWTH Aachen University
by

Sixue Wu

August 8, 2014

Department of Geoscience & Engineering · Delft University of Technology
Department of Earth Sciences · ETH Zürich
Faculty of Georesources and Material Engineering · RWTH Aachen University

Printed in The Netherlands

IDEA LEAGUE
JOINT MASTER'S IN APPLIED GEOPHYSICS

Delft University of Technology, The Netherlands
ETH Zürich, Switzerland
RWTH Aachen, Germany

Dated: *August 8, 2014*

Supervisors:	Dr. Ir. G.J.A. van Groenestijn
	Dr. Ir. G.G. Drijkoningen
Committee Members:	Dr. Ir. G.J.A. van Groenestijn
	Dr. Ir. G.G. Drijkoningen
	Dr. M. Hruska

Abstract

Blended acquisition, or simultaneous source acquisition, is a relatively new seismic acquisition design that allows shot interference. Deblending is the procedure that separates the interfering shots as if they were acquired conventionally. This thesis reviews one of the more advanced deblending algorithms in great detail, and demonstrates that it does not perform well when the source sampling is sparse.

This thesis proposes a new blended acquisition design, shot repetition, to overcome the restriction of dense source sampling by deblending solely in the common-shot domain. The theoretical fundamentals of shot repetition are derived. Based on that, three possible acquisition configurations are proposed, and the designed deblending algorithm is explained and discussed. This thesis also demonstrates that extreme noise, e.g. competitors interference and barnacle noise, can be removed by the same deblending algorithm.

The results of implementing the deblending algorithm on synthetic data of three configurations show that all the interfering shots are near-perfect separated. The results do not indicate that one configuration is better than the others. The field data results, on both blended data and the data with barnacle noise, demonstrate that strong overlapping events and weak overlapping events can be separated quite well, while the separation of strong events overlapping weak events leads to signal leakage. The deblending performance is confirmed by a significant SNR improvement on the deblended synthetic data (around $22\,dB$), a fair SNR improvement ($7\,dB$ to $12\,dB$) on the deblended field data, and a fair SNR improvement (around $5\,dB$) on the removal of barnacle noise.

Table of Contents

Chapter 1

Introduction

1-1 Exploration seismic

In our time, hydrocarbon resources are the main energy source and the source of many products like plastic, fabric, medicine, etc. In 2013, the global oil consumption grew by 1.4 per cent, which is just above the historical average since 1973 (BP statistical review of world energy, 2011). The need for hydrocarbon resources drives the exploration for hydrocarbons. Seismic exploration is the most used technique because of its penetration depth and resolution.

Seismic exploration starts by acquisition. The data acquired is converted to structural images and used to characterize the subsurface. The quality of the data and the processing techniques determine the quality of information obtained.

Conventional marine seismic acquisition

In conventional marine acquisition, sources and receivers are towed behind a vessel. Sources are airguns and receivers are a streamer (2D) or multiple parallel towed streamers (3D) of hydrophones that measure the pressure responses (Figure 1-1). In multi-component streamers, particle velocity is also measured. During one experiment in the acquisition, the vessel fires the air gun source at the target location and the hydrophones record the reflected signal. For the next experiment, the vessel tows the source to the next location and repeats the measurement.

The time between two consecutive shots is called "waiting time". The waiting time is usually kept long enough to avoid the interference from the previous shot. It is time-consuming and expensive. To economize the survey time, the current compromise is to keep the number of shots to an acceptable minimum. This leads to poor source sampling, especially in the cross-line direction.

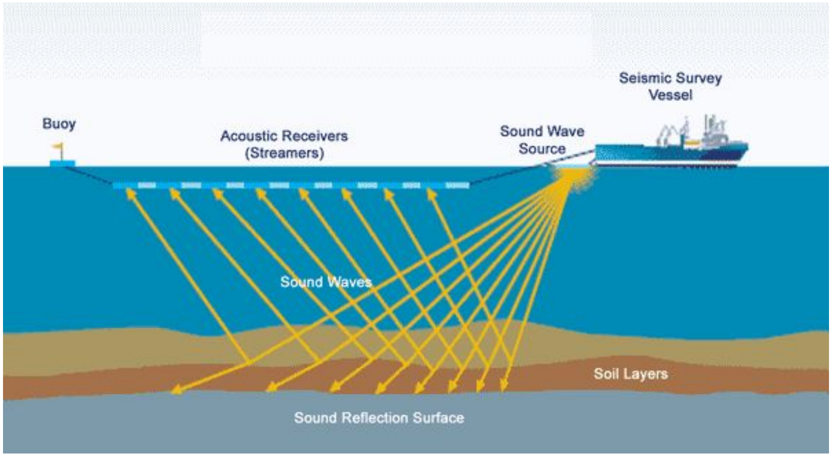

Figure 1-1: *An illustration of wave propagation paths in a 2D marine seismic survey (illustration from the website of fishsafe.eu).*

Blended marine seismic acquisition

In recent years, an acquisition design is proposed to allow shot interference (e.g. Beasley et al., 1998 and Berkhout, 2008). This is called blended acquisition or simultaneous source acquisition. More sources can be fired in the same amount of survey time (denser source sampling) so much less survey time is required for the same amount of shots. An illustration comparing the conventional acquisition with the blended acquisition is given in Figure 1-2.

The existing processing scheme in the industry is developed for data of one source wave field. It will take a lot of effort to adjust every processing technique such that it can handle the blended data. The current solution for blended data is to first separate interfering shot records as if they were acquired conventionally. This process is called deblending. Deblending is regarded as a preprocessing step so that the traditional processing scheme can be followed.

1-2 Literature review on deblending

The essence of the blended acquisition is to design a survey in a way that it can be deblended. The simultaneous firing of sources is a well established land acquisition technique (e.g. Womack et al., 1990). Simultaneous impulse sources in marine acquisition are less well explored.

Beasley et al. (1998) first introduced the use of simultaneous source in marine acquisition. Two airgun sources are placed symmetrically at the end of a 2D marine cable and fired simultaneously. This results in two shot records in one gather that dip in opposite directions. A geometry-related filter can separate the shots based on the opposite dips.

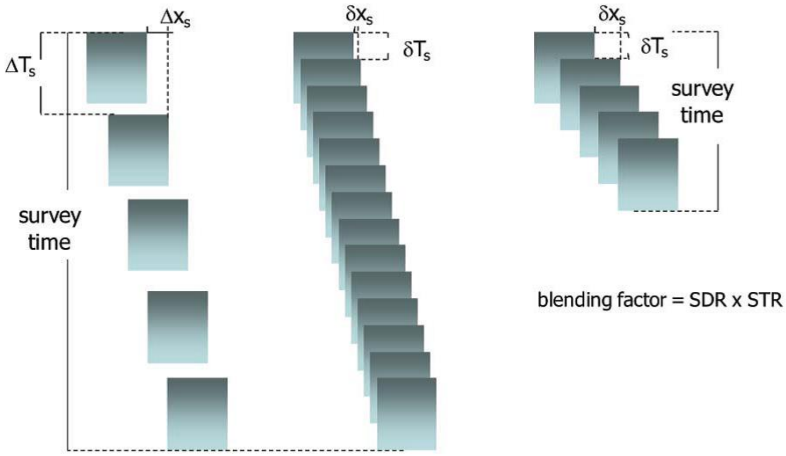

Figure 1-2: *(left) Conventional seismic acquisition without blending. (center) Blending with focus on dense source sampling. (right) Blending with focus on survey time: for the same source spatial sampling, the survey time can be significantly reduced. ΔT_s and Δx_s are the time interval between two consecutive shots, and the source spacing in a conventional survey. δT_s and δx_s are the time interval and source spacing of a blended survey (illustration from Berkhout (2008)).*

Vaage (2002) proposed to apply random firing time sequences to the blended sources. Each of the firing sequences includes firing of the first source, and waiting a selected time before firing the second source. The selected time between the two near-simultaneous sources is different in every experiment. In this way, the signal originated from the first source can be identified from the second source in any other domains except the common-shot domain.

Deblending can be considered as a denoising problem. The interference due to blending is regarded as noise. Many authors have suggested a deblending method based on a prediction and subtraction scheme (e.g. Spitz et al., 2008 and Mahdad et al., 2011).

There are two strategies for deblending in the above scheme. One strategy is to resort data in another domain besides the common-shot domain and apply the coherency constraint. The method of Mahdad et al. (2011) falls in this category and will be discussed in detail in Chapter 2. The other strategy is to convert the data in a transferred domain and use the sparsity to invert for the unblended data. For instance, the transferred domain can be the linear or hyperbolic Radon domain, or the double focal domain, e.g. the method of Kontakis and Verschuur (2014).

Some discussed the limitation of the deblending method based on the random source firing acquisition. When the poor source sampling causes spatial aliasing, the deblending method fails to give satisfying results. In this case, no filter can distinguish the direction of wave propagation to successfully remove the interference. This limits the acquisition design with respect to the source spacing.

This thesis proposes a new blended acquisition design that uses shot repetition. This avoids the dense source sampling restriction. The design of this acquisition is aimed at separating blended shots in the shot domain. So there are no restrictions on the source sampling interval.

1-3 A new survey design - shot repetition

In both a conventional and a traditional blended seismic survey, each shot location is only visited once by a source. This thesis proposes a new acquisition design - shot repetition. A shot-repetition survey refers to a blended survey where a source is fired more than one time at the same location. The time interval between the repeated shots can be designed to be larger than the waiting time to avoid blending or small to allow blending.

Shot repetition can be designed in many configurations. In this thesis, I tested three shot-repetition configurations for blended acquisition, and two special scenarios; barnacle noise and competitor shooting. The three acquisition configurations and their shot gathers are illustrated in Figure 1-3. The stars above the shot gathers indicate the source locations and firing time. Note that the straight lines that wrap around the reflection edges are artifacts in the synthetic data.

It will be demonstrated in this thesis that, with the help of double information at one location, individual shots can be obtained from these three configurations. This makes deblending shots in the common-shot domain possible. Hence there is no restriction on dense source sampling. Shot repetition also makes it possible to enhance the data quality in the presence of strong noise, as will be demonstrated in the case of barnacle noise in Chapter 4.

1-4 Thesis outline

The main focus of this thesis is to present how to deblend shot-repetition data. This thesis consists of the following chapters:

Chapter 2: *The forward model of shot repetition and domain-switching deblending.*
This chapter introduces the matrix representation of seismic data (Berkhout, 1982) and the source blending concept (Berkhout, 2008). The forward model of shot repetition is based on source blending. The domain-switching deblending methods are introduced. The deblending method of Mahdad et al. (2011) is discussed in detail and its limitation is discussed.

Chapter 3: *Deblending by shot repetition.*
This chapter presents how to deblend shot-repetition data. The practical steps of the method are given. Synthetic data are used to illustrate the steps and the deblending results. The type-II configuration, as defined in Chapter 1, is used to introduce the

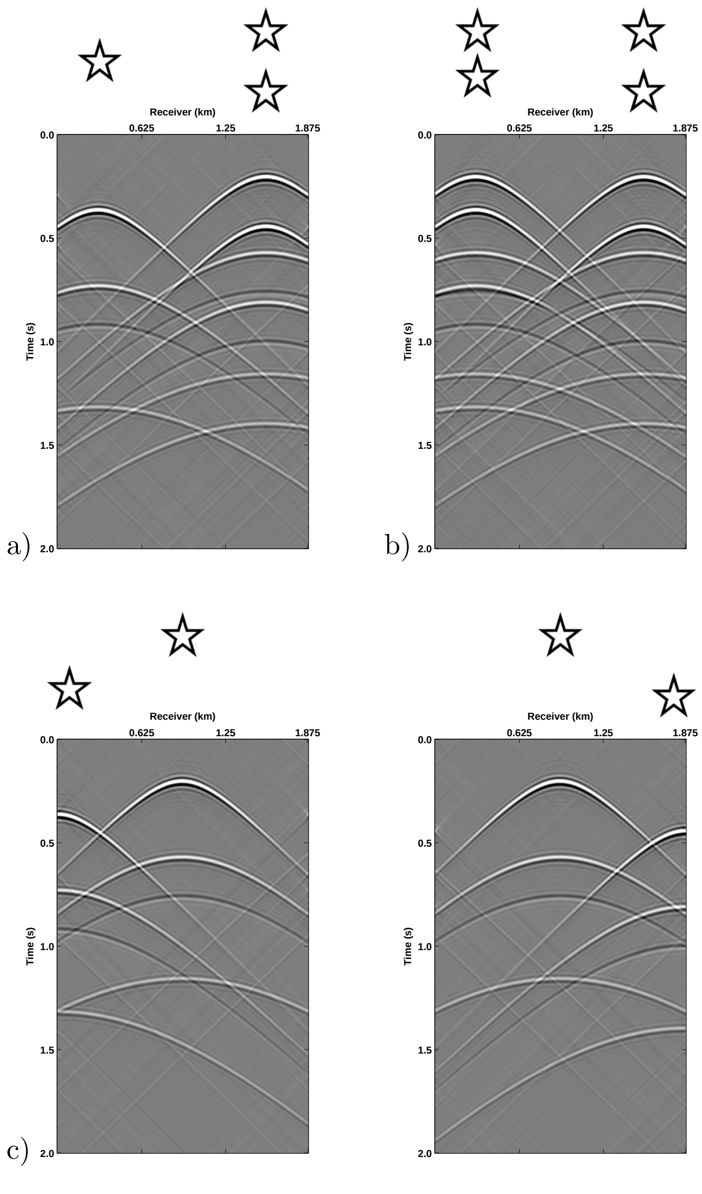

Figure 1-3: *Three shot-repetition configurations for blended acquisition:* **(a)** *type-I: 3 shots in one gather,* **(b)** *type-II: 4 shots in one gather,* **(c)** *type-III: 3 shots in 2 gathers.*

method. Insights of deblending data of type-I and type-III configurations are given. It is also demonstrated that, in the special case of uncontrolled source deblending, can be useful.

Chapter 4: *Field data examples.*
In this chapter, numerically blended field data in the three different configurations are used to test the algorithm. The algorithm is also tested for data with barnacle noise. Deblending results are discussed.

Chapter 5: *Discussion and conclusions.*
This chapter summarizes the main conclusions and discusses the future plans.

Chapter 2

The forward model of shot repetition and domain-switching deblending

2-1 Seismic modelling of conventional data

The goal of seismic processing is to extract structural images from acquired seismic data. This is an inverse problem. To solve it, a forward model is needed. The forward model describes the physical processes that happen in a seismic experiment, i.e. from source input to receiver recording in the subsurface. In this thesis, I use the wave field extrapolation based model of Berkhout (1982), to build the forward model of unblended and blended data.

2-1-1 The data matrix

In conventional seismic acquisition, the response recorded by one receiver from one source is one trace. In the 2D case, all the recorded traces can be arranged in a data cube by their source and receiver positions (see Figure 2-1). After a Fourier transform along the time axis, one frequency slice of this data cube is the so-called data matrix **P**.

Each element of **P** is a complex valued number that represent one frequency component of a recorded trace. Each column of **P** represents a monochromatic shot gather, each row represents a receiver gather, each diagonal represents a common-offset gather, and each anti-diagonal represents a common-midpoint gather (see Figure 2-2).

2-1-2 Matrix representation of seismic data

The data matrix, **P**, can be decomposed into a matrix multiplication of three matrices:

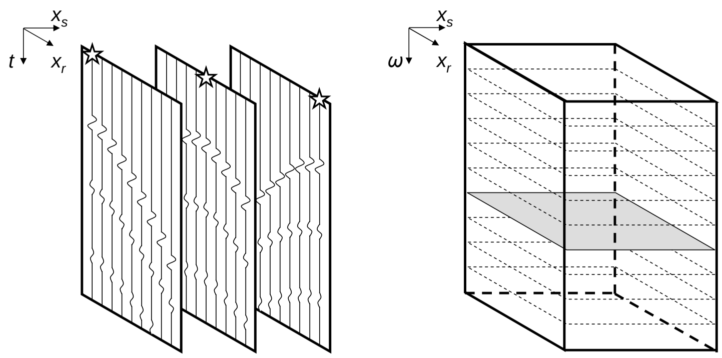

Figure 2-1: *Illustration of the data matrix (from van Groenestijn (2010)).*

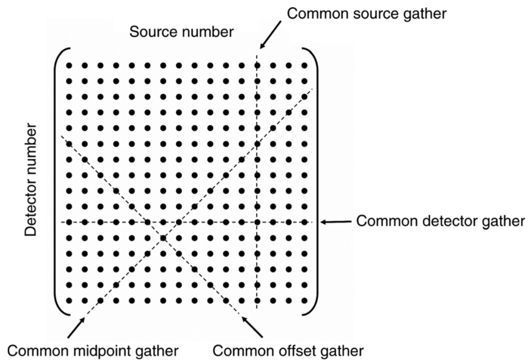

Figure 2-2: *The schematic data matrix (from Mahdad et al. (2011).*

$$\mathbf{P} = \mathbf{DXS}. \tag{2-1}$$

A schematic plot of Equation 2-1 is shown in Figure 2-3.

S represents the source matrix. Each column of the source matrix corresponds to the experiment index, and each row corresponds to the lateral source position in the survey. Conventionally, there is only one non-zero entry in each column of the source matrix, due to a single source in an experiment. An example of a source matrix in a conventional survey design is given in Figure 2-4 a. Each red star indicates a source wave field at each location.

X represents the multi-dimensional transfer function of the earth. It contains the entire subsurface response, including primaries, multiples, surface waves, etc.

D represents the receiver array matrix. It transforms the earth response wave field into the measured wave field. It includes the operator that generates the receiver ghost.

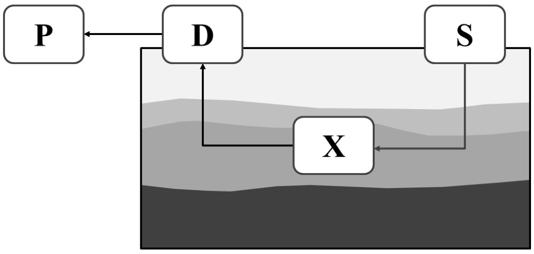

Figure 2-3: *The system representation of seismic data.*

2-2 The concept of source blending

In a blended seismic experiment, the forward model should be adjusted due to the change of the source configuration. Berkhout (2008) showed the concept of source blending. The source matrix of a blended seismic acquisition is given by:

$$\mathbf{S}_{bl} = \mathbf{S}\mathbf{\Gamma}, \tag{2-2}$$

$\mathbf{\Gamma}$ is the blending operator that manipulates the source matrix $\mathbf{S}$. Each non-zero element of the matrix $\mathbf{\Gamma}$, $\mathbf{\Gamma}_{kl}$, applies the time delay Δt_{kl} to source k in blended experiment l;

$$\mathbf{\Gamma}_{kl} = e^{-j\omega\Delta t_{kl}}. \tag{2-3}$$

Figure 2-4 b shows an example of the blending matrix $\mathbf{\Gamma}$, and the matrix operation of source blending. An element of $\mathbf{\Gamma}$ that equals one, indicates that no time delay is applied to the source ($e^{-j\omega\Delta t_{kl}} = 1$, when $\Delta t_{kl} = 0$). The blended source matrix, $\mathbf{S}_{bl}$, has less columns than the unblended source matrix $\mathbf{S}$. Physically, $\mathbf{S}_{bl}$ conveys less experiments for the same amount of shots.

Substituting Equation 2-2 in Equation 2-1, the blended seismic data can be modeled as:

$$\mathbf{P}_{bl} = \mathbf{D}\mathbf{X}\mathbf{S}_{bl} = \mathbf{P}\mathbf{\Gamma}. \tag{2-4}$$

A similar matrix operation as shown in Figure 2-4 b is performed on the monochromatic data matrix $\mathbf{P}$. The blending operator only changes the source matrix. The receiver operator $\mathbf{D}$ and the transfer function $\mathbf{X}$ are not affected.

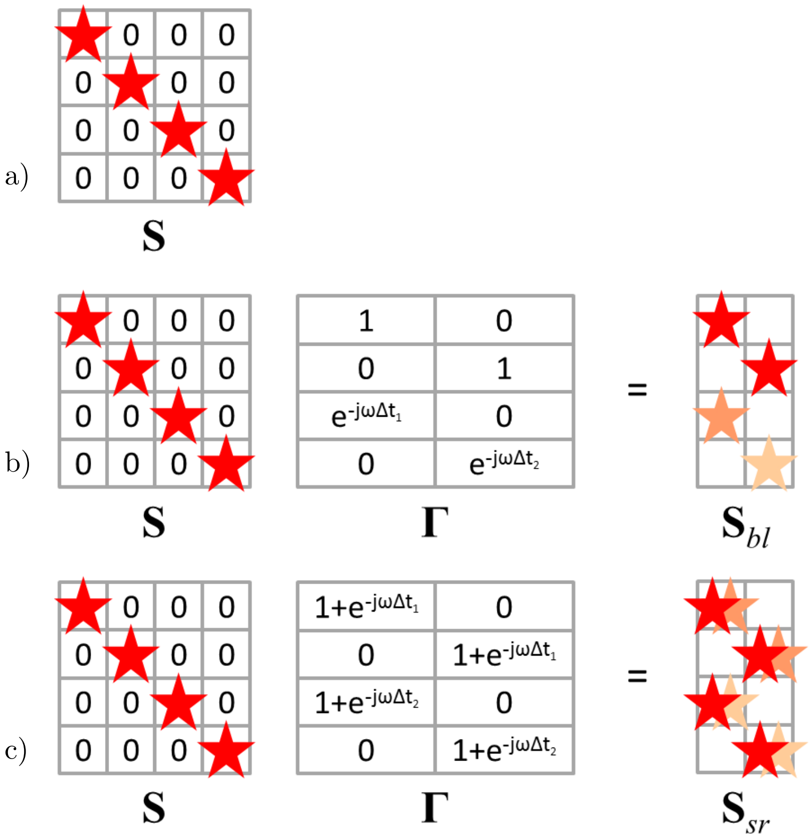

Figure 2-4: *Schematic plots of different source matrices.* **(a)** *in a conventional acquisition,* **(b)** *in a traditional blending acquisition,* **(c)** *in a shot-repetition acquisition.*

2-3 Shot repetition

In shot repetition, the sources are blended in both the spatial axis and the time axis. In this special case of blending, the non-zero elements of the blending matrix can be formulated as:

$$\mathbf{\Gamma}_{kl} = e^{-j\omega\Delta t_{kl,1}} + e^{-j\omega\Delta t_{kl,2}}, \tag{2-5}$$

The source code is the sum of two phase terms. $e^{-j\omega\Delta t_{kl,1}}$ corresponds to the time delay of the first shot, and $e^{-j\omega\Delta t_{kl,2}}$ corresponds to the time delay of the second shot. Note that, both shots are at the same location.

The forward model of shot repetition can be formulated as:

$$\mathbf{P}_{sr} = \mathbf{P}\mathbf{\Gamma}, \tag{2-6}$$

with the non-zero elements of the Γ matrix given by Equation 2-5.

Note that Equation 2-6 has the same form as Equation 2-4, with the blending matrix Γ different. Figure 2-4 c shows the matrix operation of shot repetition. It is illustrated for type-II shot-repetition configuration. A shot gather in this configuration is given in Figure 1-3.

2-4 Domain-switching deblending methods

Many deblending methods have been developed based on randomized firing time. These methods require resorting data in any other domain than the shot domain. Hence, I call methods of this type domain-switching deblending methods. In this section, the method of Mahdad et al. (2011), as an example of the domain-switching methods, will be discussed in detail. Understanding this method is beneficial for understanding deblending by shot repetition.

The deblending process can be seen as a denoising problem, where the interference due to blending is considered noise. This blending noise can be modeled by Equation 2-4 and subtracted from the blended data iteratively. I will first introduce the blended synthetic data, and introduce the method step by step. A flowchart of the iterative algorithm is given in Figure 2-5.

The blended data

A synthetic blended data set (2D) with dense spatial sampling are used to illustrate the deblending method. The temporal and spatial sampling interval for this example are $4\,ms$ and $12.5\,m$, respectively. A shot gather from the blended data (Figure 2-6 a) shows interfering shots and has 150 traces. A receiver gather from the blended data (Figure 2-6 b) shows one aligned shot and has only 75 traces. Note that the spacial coordinate of the receiver gather indicates the experiment index. In a conventional survey, the experiment number is equivalent to source number.

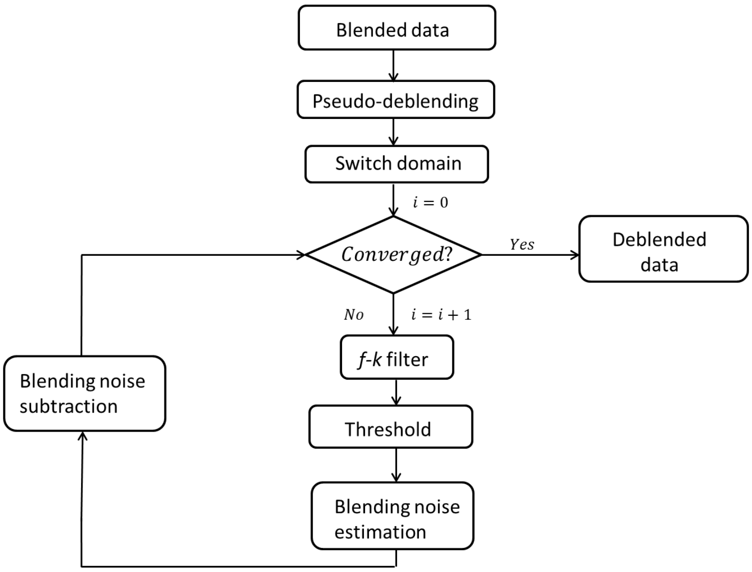

Figure 2-5: *The flowchart of a domain-switching deblending algorithm.*

In general, the size of the blended data matrix is $\frac{1}{b}$ of the size of the unblended data matrix. b is the number of shots blended in one experiment. There are two sources blended in this example ($b = 2$). The receiver gather shows that the number of blended experiment is the half of the unblended case.

Pseudo-deblending

Deblending is an underdetermined inverse problem, so there is no unique solution. Since seismic data is physical, the inversion can be constrained to obtain a realistic solution. Mathematically, a minimum energy solution to the deblending problem can be calculated and the inverse of the blending matrix $\mathbf{\Gamma}$ can be formulated as:

$$< \mathbf{\Gamma}^{-1} >= [\mathbf{\Gamma}^H \mathbf{\Gamma}]^{-1} \mathbf{\Gamma}^H. \tag{2-7}$$

$\mathbf{\Gamma}^H$ is the transposed complex conjugate (Hermitian) of $\mathbf{\Gamma}$. When the blending matrix $\mathbf{\Gamma}$ only contains phase terms, and the number of blended sources in every experiment is constant, the pseudo-inverse of $\mathbf{\Gamma}$ can be approximated as $\mathbf{\Gamma}^H$. In this special case, pseudo-deblending can be formulated as:

$$\mathbf{P}_{ps} = \mathbf{P}_{bl} \mathbf{\Gamma}^H. \tag{2-8}$$

Physically, pseudo-deblending copies each blended shot gather b times, and corrects each copy for the time delay of each source. Figure 2-7 a shows a pseudo-deblended shot gather (one column of the pseudo-deblended data $\mathbf{P}_{ps}$) and its *f-k* spectrum. Both shots are coherent in the gather and all the signal resides in the *f-k* signal cone. Note that, in Figure 2-7, only the deblending of the left shot is shown. The deblending of the right shot has the same behavior.

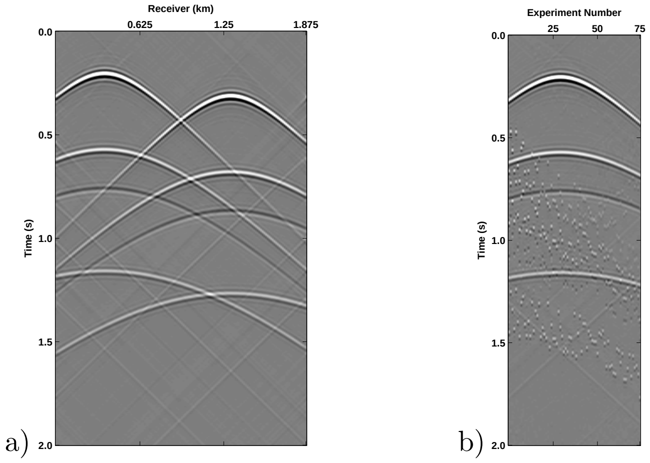

Figure 2-6: **(a)** *One column of the blended data matrix.* **(b)** *One row of the blended data matrix.*

Switching domain

The pseudo-deblended data, $\mathbf{P}_{ps}$, is resorted in a different domain than the shot domain. Mahdad et al. (2011) shows that the aligned shots are coherent while all the other shots are incoherent in the switched domain, e.g. common-receiver gather or common-offset gather. As an example, Figure 2-7 b presents one receiver gather (one row in the matrix) extracted from the pseudo-deblended data. It can be observed that $\mathbf{P}_{ps}$ now has the same size as the unblended data. In the following, the receiver gather is continuously used to illustrate the steps. Note that the incoherent nature of the interfering shots in another domain is the discriminating power for the domain-switching deblending methods.

f-k filter

An *f-k* filter is used as a coherency constraint. It is applied to every receiver gather of the first deblending estimate $\mathbf{P}_{ps}$. The *f-k* filter attenuates the incoherent events while the coherent events keep the same amplitude. This is because the *f-k* domain of the incoherent events have a white spectrum. The *f-k* filter mutes the energy spreading out of the signal cone. See Figure 2-7 b and Figure 2-7 c.

Note that, the incoherent energy that resides in the *f-k* signal cone cannot be removed.

Thresholding

After *f-k* filtering, the coherent events have higher amplitudes than the incoherent events. To form an unblended estimate that only contains energy from the coherent events, a threshold in the x-t domain that passes parts of the signal that have amplitudes higher than an iterative threshold value. The samples that have values lower than the threshold are set to zeros. For example, the initial threshold value can be chosen as 95% of the maximum amplitude in the blended shot gather, then it is lowered at each iteration. The value of threshold is lowered to zero in the last iteration such that every event in the data will be used in the end.

Ideally, no blending noise is present after thresholding. Threshold operates on individual samples which are composed of various frequency components. Thus, thresholding aids the f-k filter to better remove the incoherent energy. The output of this step is the estimated unblended part of the data and is noted as $\bar{\mathbf{P}}_i$.

Modeling blending noise

The unblended estimate $\bar{\mathbf{P}}_i$ is used to predict part of the blending noise $\hat{\mathbf{N}}_i$ at each iteration step. It can be formulated as:

$$\hat{\mathbf{N}}_i = \bar{\mathbf{P}}_i \boldsymbol{\Gamma} \boldsymbol{\Gamma}^H - \bar{\mathbf{P}}_i. \tag{2-9}$$

$\bar{\mathbf{P}}_i \boldsymbol{\Gamma} \boldsymbol{\Gamma}^H$ models the pseudo-deblended $\bar{\mathbf{P}}_i$, which contains both the desired signal and the blending noise. Subtracting $\bar{\mathbf{P}}_i$, the desired signal, leaves only the blending noise.

Blending noise subtraction

The blending noise $\hat{\mathbf{N}}_i$ is subtracted from the pseudo-deblended data $\mathbf{P}_{ps}$. The output of this step, $\hat{\mathbf{P}}_i$, is considered the deblending estimate and is used in the beginning of each iteration (Figure 2-5). $\hat{\mathbf{P}}_i$ can be formulated as:

$$\hat{\mathbf{P}}_i = \mathbf{P}_{ps} - \hat{\mathbf{N}}_i \tag{2-10}$$

Iteration

The pseudo-deblended data $\mathbf{P}_{ps}$ is used as the first deblending estimate ($\hat{\mathbf{P}}_{i=1}$) in the iteration scheme. Afterwards, the deblending estimate, $\hat{\mathbf{P}}_i$, is updated at each iteration, while the pseudo-deblended data, $\mathbf{P}_{ps}$, does not change during the iteration. Examples of the output after each step are given in Figure 2-7.

Figure 2-8 shows the deblending estimate $\hat{\mathbf{P}}_i$ after 10, 25, and 28 iterations. Only the deblending of the left shot is shown. The deblending of the right shot has the same behavior. A gradual removal of the blending noise in the receiver gather can be observed. Comparing the deblending result with the unblended data, it is clear that the domain-switching deblending method works well for deblending well sampled synthetic data.

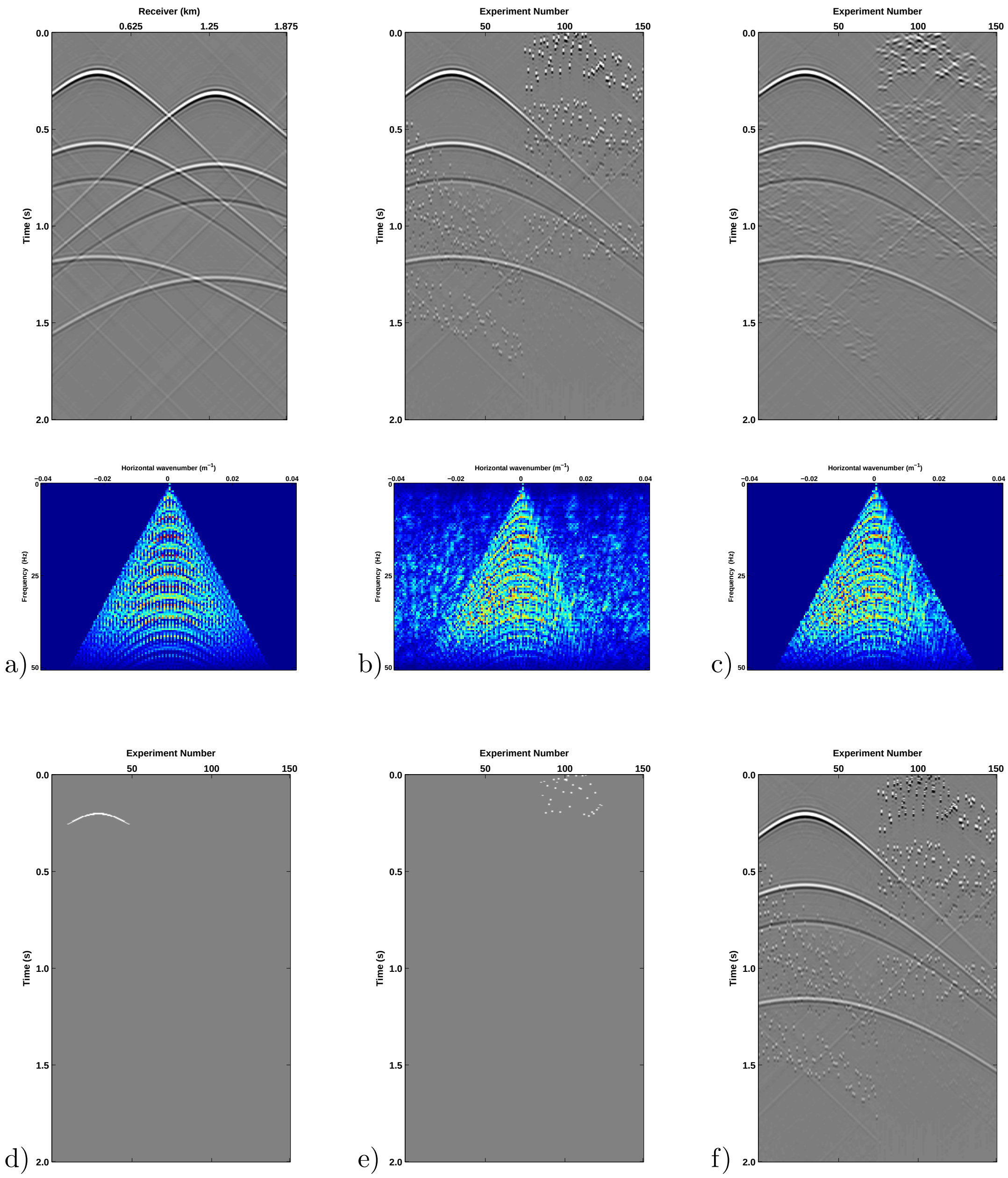

Figure 2-7: *Example output after each step.* **(a)** *A shot gather of the pseudo-deblended data,* $\boldsymbol{P}_{ps}$*, and its f-k spectrum.* **(b)** *A receiver gather of the pseudo-deblended data,* $\boldsymbol{P}_{ps}$*, and its f-k spectrum.* **c)** *A receiver gather after f-k filter, and its f-k spectrum, at iteration 1.* **d)** *After threshold.* **e)** *Modeled blending noise.* **f)** *Subtract noise from* $\boldsymbol{P}_{ps}$*.*

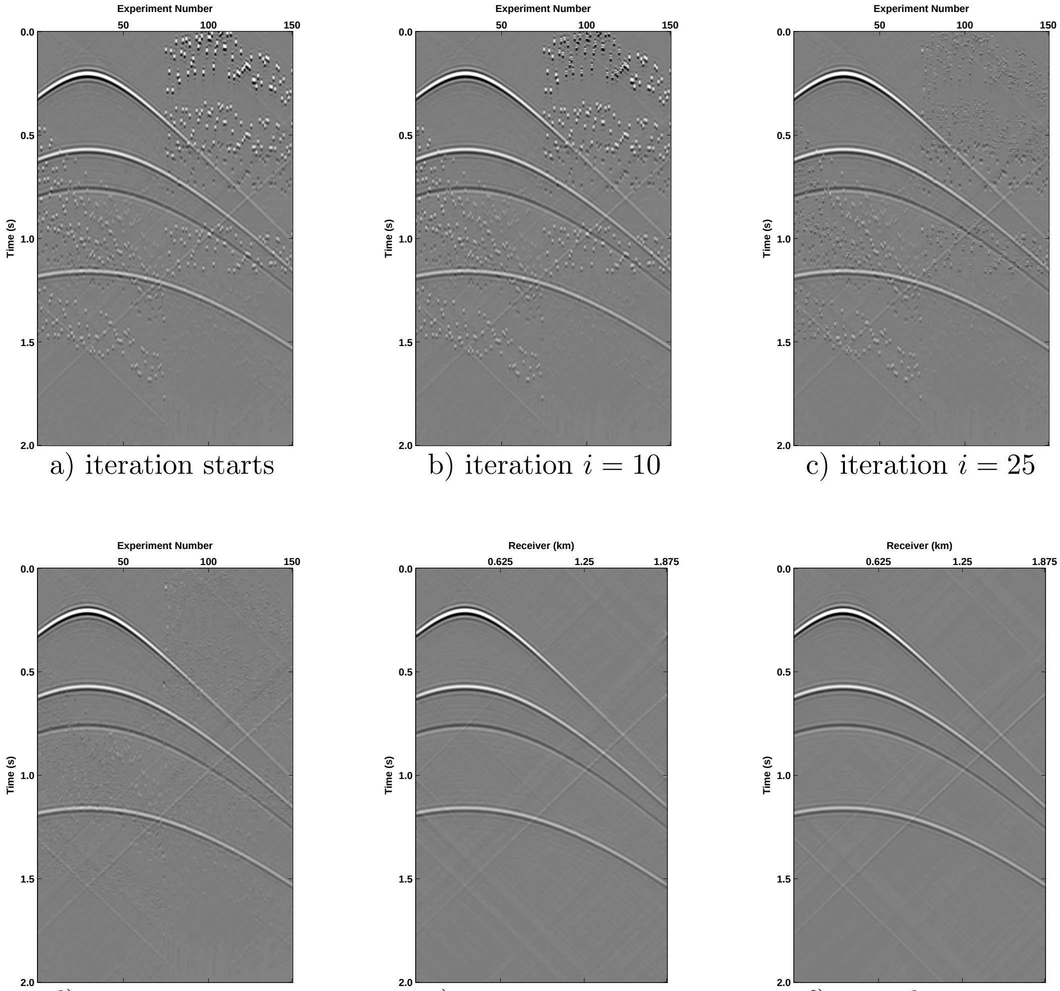

a) iteration starts b) iteration $i = 10$ c) iteration $i = 25$

d) iteration $i = 28$ e) iteration $i = 30$ f) true shot

Figure 2-8: *The deblending estimate, $\hat{\boldsymbol{P}}_i$, at certain iterations.* **(a)** *A receiver gather of the first deblending estimate, $\boldsymbol{P}_{ps}$.* **(b)** *A receiver gather of $\hat{\boldsymbol{P}}_i$ at iteration 10,* **(c)** *at iteration 25,* **(d)** *at iteration 28,* **(e)** *and the final deblended shot at iteration 30.* **(f)** *The true unblended shot.*

2-5 The limitation of the domain-switching deblending methods

The blended acquisition of Vaage (2002) and the domain-switching deblending methods work well and are well accepted by the industry. Studies on these methods show that it requires a dense source sampling. In this section, I will demonstrate what happens when this requirement is not met.

The synthetic data shown in the previous section have a shot spacing of $12.5\,m$. Now I increase the shot spacing to $50\,m$, four times the previous source spacing. The number of traces in the common-receiver gather is reduced to one quarter of the previous one.

I use the domain-switching deblending method to deblend this poorly sampled data. Figure 2-9 a shows that one shot gather of the pseudo-deblended data is smooth in the x-t domain and not aliased in the f-k domain. However, one receiver gather of the pseudo-deblended data shows visible steps in the coherent events in the x-t domain, while spatial aliasing in the f-k domain (Figure 2-9 b).

Due to the large source spacing, the Nyquist wavenumber is reduced to $0.01\,m^{-1}$, one quarter of the previous case. A new f-k filter in Figure 2-10 b is designed to keep all the data in the signal cone; the highest frequency that it can filter is around $20\,Hz$. After a Fourier transformation back to the x-t domain, parts of the blending noise keep high amplitudes (Figure 2-10 b), because the high-frequency components of the blending noise remain in the data. The power of the f-k filter, as a coherency constraint, is strongly degraded.

After thresholding, the high amplitude blending noise can be selected together with the desired signal. This leads to noise leaking to the estimation of the desired shot at each iteration. In the final deblending results, the interfering shots are not strongly presented but also not completely removed. See Figure 2-11.

I conclude that large source spacing limits the performance of the domain-switching deblending by inducing severe spatial aliasing. Using a different deblending algorithm, Peng et al. (2008) also showed results clearly indicating that increasing source spacing degrades the deblending results.

2-6 Remarks on the domain-switching deblending

The domain-switching deblending method and its limitation is discussed in the previous two sections. Several remarks on this method are given below.

Regarding deblending as an ill-posed inversion problem, it is impossible to converge to an unique solution. But it is possible to find a solution which is closest to reality, by taking advantages of the physical constraints of the seismic data. By giving the minimum energy solution, $\mathbf{P}_{ps}$, the iteration is brought to start from a physical point. The physical constraints

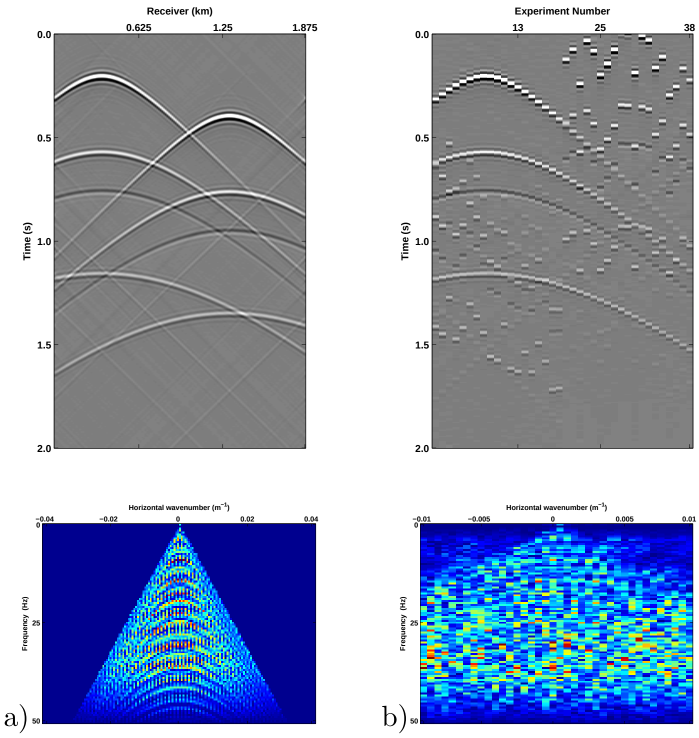

Figure 2-9: *Pseudo-deblended data, and their corresponding f-k spectra, with shot spacing of* $50\,m$. **(a)** *A shot gather (one column of* $\boldsymbol{P}_{ps}$*),* **(b)** *A receiver gather (one row of* $\boldsymbol{P}_{ps}$*).*

make sure that the inversion converges to the right direction.

The physical constraints that have been imposed in deblending are discussed below:

- Unblended seismic data remains physical when it is sorted to another domain. Therefore, one can make advantages of the incoherent firing time of sources in blended seismic data.

- Seismic data is coherent in various domains because it represents interfaces in the subsurface. The coherency constraint is implemented to separate the coherent and incoherent events to converge to a realistic result. However, the separation is usually not strong enough. Therefore, a threshold is used to aid the removal of incoherent energy and it works well. The drawback of threshold, is that it causes signal leakage.

If the coherency pass filter is strong enough to separate all the coherent and incoherent events, one does not need a thresholding process. A better tool that filters part of the coherent events than a simple threshold might performs better on this process.

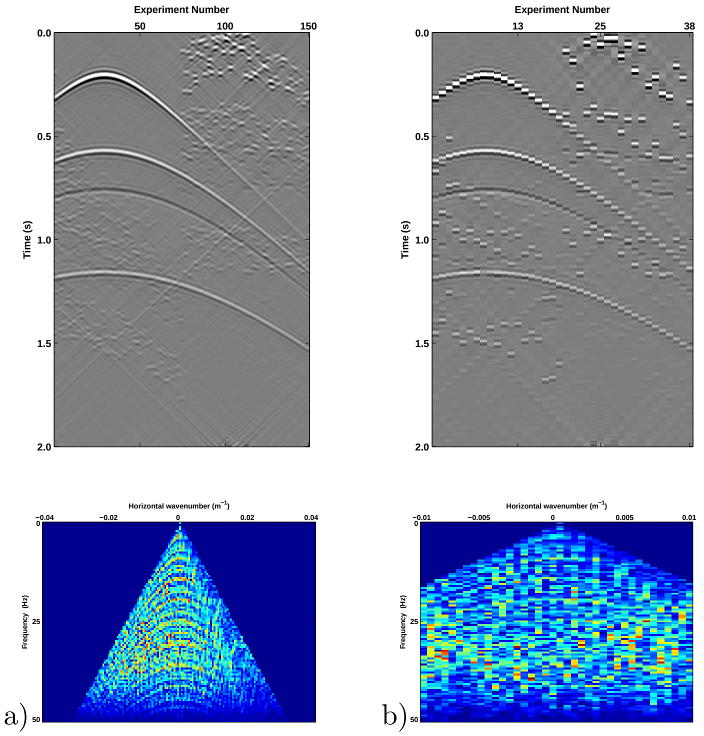

Figure 2-10: *Output after f-k filters, and their corresponding f-k spectra, when* **(a)** *source spacing is* $12.5\,m$*,* **(b)** *source spacing is* $50\,m$*.*

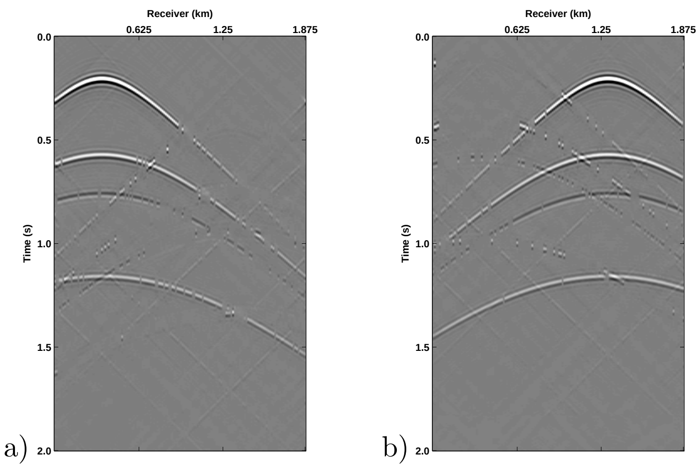

Figure 2-11: *The final deblended results, after 100 iterations (with shot spacing* $50\,m$*).*

Chapter 3

Deblending by shot repetition

3-1 Deblending method

Deblending by shot repetition aims at retrieving individual shots from shot-repetition data as if they were acquired conventionally. The deblending process is an underdetermined inverse problem, because the shot-repetition data, $\mathbf{P}_{sr}$, has fewer columns than $\mathbf{P}$. There is no unique solution to the problem. But additional constraints can be introduced to drive the solution closer to the reality.

The approach of deblending by shot repetition follows the same lines as in the noise estimation and subtraction scheme as the deblending method introduced in Section 2-4. To deblend data only in the shot domain, I use a technique called random-sample selection to benefit from the nature of the repeating shots. An overview of the method is given in the flowchart in Figure 3-1.

The shot-repetition data

The shot-repetition data used for deblending is numerically blended by the same synthetic data introduced in section 2-4. A shot gather extracted from the shot-repetition data is shown in Figure 3-2. The shot-repetition data belongs to the type-II configuration, as introduced in Chapter 1. The shot gather contains four shots in total. The left sources are fired at $0.0\,s$ and $0.16\,s$, and the right sources at $0.0\,s$ and $0.24\,s$. Note that, the differences in firing times of the left and right shots are different; $0.16\,s$ and $0.24\,s$.

I will use this blended shot gather to illustrate deblending by shot repetition. The method consists of six steps.

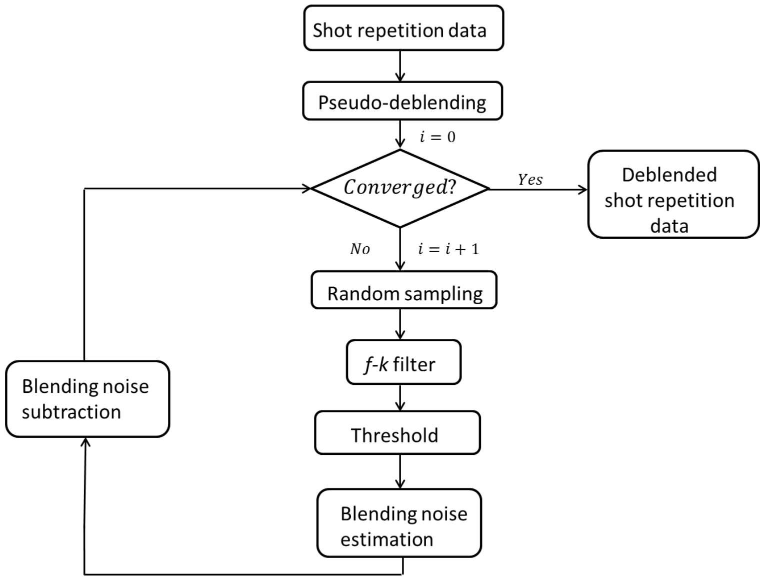

Figure 3-1: *The flowchart of deblending by shot repetition.*

Pseudo-deblending

The formulation of pseudo-deblending in the shot-repetition case is slightly different from the blending case in Section 2-4. The $\mathbf{\Gamma}$ matrix is first replaced by a multiplication of two matrices;

$$\mathbf{\Gamma} = \mathbf{\Gamma}_A \mathbf{\Gamma}_B. \tag{3-1}$$

When $\mathbf{\Gamma}_A \mathbf{\Gamma}_B$ is multiplied with a source matrix, $\mathbf{\Gamma}_A$ will double the number of columns of the source matrix it operates on, and $\mathbf{\Gamma}_B$ will apply the right time shift to each column, and blend the columns together in the end. An example of matrix operation in Equation 3-1 is illustrated below:

If

$$\mathbf{\Gamma} = \begin{bmatrix} 1 + e^{-j\omega\Delta t_1} \\ 0 \\ 1 + e^{-j\omega\Delta t_2} \\ 0 \end{bmatrix} \quad ,$$

then

$$\mathbf{\Gamma}_A = \begin{bmatrix} 1 & 1 & 0 & 0 \\ 0 & 0 & 0 & 0 \\ 0 & 0 & 1 & 1 \\ 0 & 0 & 0 & 0 \end{bmatrix} \quad ,$$

and

$$\mathbf{\Gamma}_B = \begin{bmatrix} 1 \\ e^{-j\omega\Delta t_1} \\ 1 \\ e^{-j\omega\Delta t_2} \end{bmatrix} \quad .$$

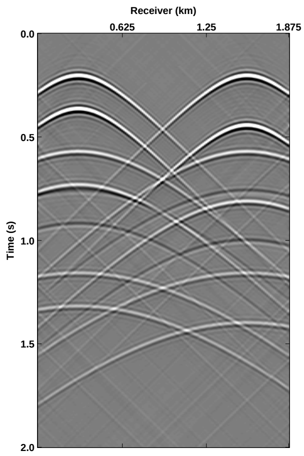

Figure 3-2: *A shot gather extracted from the shot-repetition data.*

After introducing the $\mathbf{\Gamma}_A$ and $\mathbf{\Gamma}_B$ matrix, the pseudo-deblended shot-repetition data can be formulated as:

$$\mathbf{P}_{ps} = \mathbf{P}_{sr}\mathbf{\Gamma}_B^H \tag{3-2}$$

Physically, $\mathbf{\Gamma}_B^H$ copies the blended data and removes the time delay of each shot. Figure 3-3 shows the four pseudo-deblended shot gathers. Note that if $\mathbf{\Gamma}^H$ would be applied to $\mathbf{P}_{sr}$ instead of $\mathbf{\Gamma}_B^H$, there would have been only two gathers instead of four in Figure 3-2.

Pseudo-deblending aligns one shot to its repetition. The shots pointed by arrows in Figure 3-3 a and b are seen as identical. Similarly, the arrow pointed shots in Figure 3-3 c and d are seen as identical.

Random-sample selection

The aligned shots in the pseudo-deblended data are the desired events. I form two new gathers by selecting samples from the four gathers in Figure 3-3, so that the aligned event stays the same while all the other events becomes incoherent (Figure 3-4). Note that sample selection has transformed the four pseudo-deblended gathers in two gathers. There are many realizations for forming the new gathers. Here, I select every three other traces for better illustration. However, I learned from experience that the best result returns when random samples are selected. Note that the coherent and the incoherent events in Figure 3-4 have the same strength, in terms of amplitude.

This step differs with the domain-switching deblending method. Instead of switching domain, random-sample selection arranges the physical events in the shot gathers where a coherency constraint can be applied. It is solely an operation in shot gathers, therefore it does not require dense source spacing.

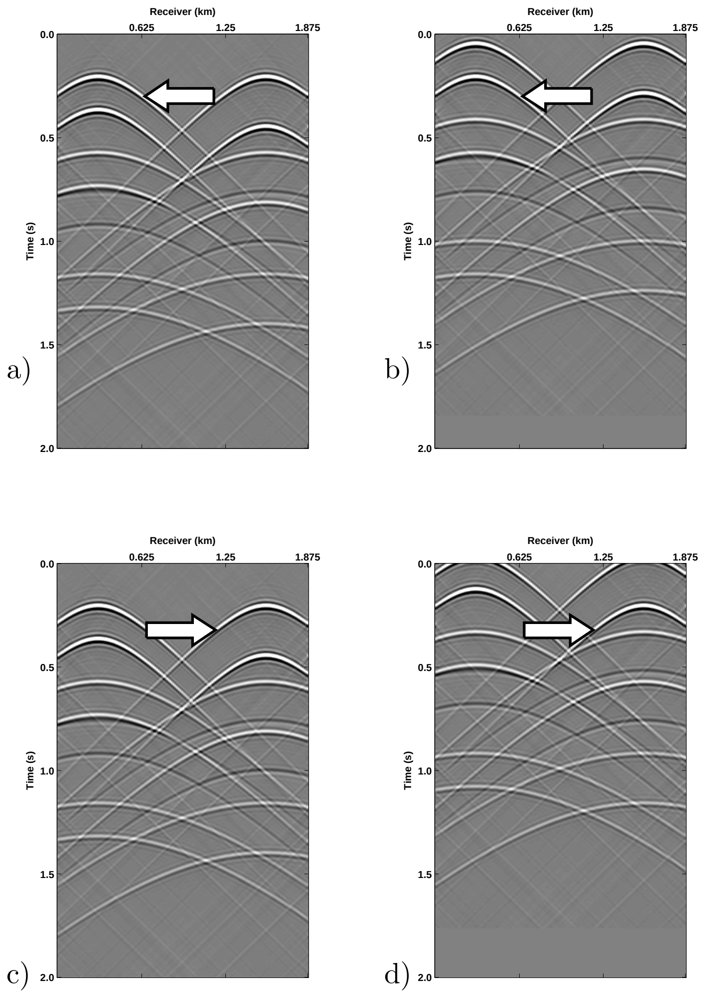

Figure 3-3: *Shot gathers after pseudo-deblending:* **(a)** *corrected for the time delay of the first left shot (*$0.0\,s$*),* **(b)** *corrected for the time delay of the second left shot (*$0.16\,s$*),* **(c)** *corrected for the time delay of the first right shot (*$0.0\,s$*),* **(d)** *corrected for the time delay of the second right shot (*$0.24\,s$*).*

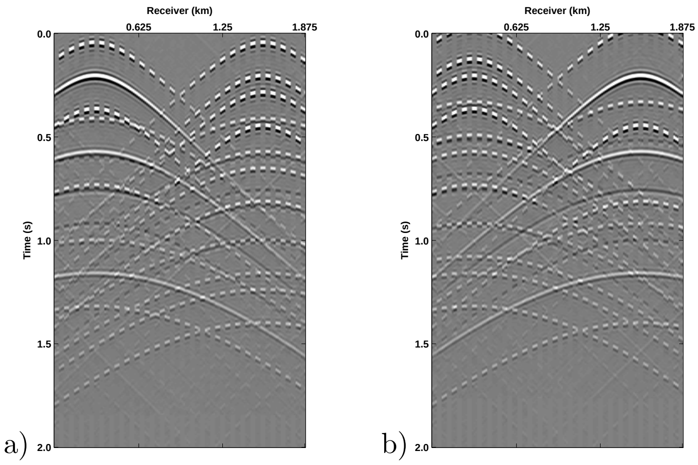

Figure 3-4: *Shot gathers after sample selection,* **(a)** *aligned for the left shot,* **(b)** *aligned for the right shot.*

f-k filter

A simple *f-k* filter is implemented as a coherency constraint. It keeps parts of the data that resides in the *f-k* signal cone. The incoherent energy that extends out of the *f-k* signal cone will be removed. Hence, the incoherent events are attenuated and the highest amplitude belongs to the coherent event. The shape of the *f-k* filter is designed based on the steepest dipping event in the seismic data, i.e., the water bottom reflection. The *f-k* spectra in Figure 3-5 b shows the shape of the *f-k* filter. After a Fourier transformation back to the x-t domain, the incoherent events have a lower strength than the coherent events, as can be clearly observed by comparing Figure 3-5 a and b.

Note that, the blending noise that mixed in the signal cone cannot be removed. To be able to remove this part of the incoherent energy, we need the help of the next steps.

Thresholding

In order to form an unblended estimate that only contains energy from the coherent events, I apply a threshold in the x-t domain that passes only part of the signal that have amplitudes higher than an iterative threshold value. For example, the initial threshold value can be chosen as 95% of the maximum amplitude in the blended shot gather. It is lowered at each iteration. The value of threshold is lowered to zero in the last iteration such that every event in the data will be used in the end. Figure 3-6 a and d show the signal passed the threshold, i.e. the unblended estimate, at a certain iteration. The unblended estimate at each iteration is noted as $\bar{\mathbf{P}}_i$.

Ideally, after thresholding only the coherent signal is picked, because the amplitude of the blending noise went down after the f-k filter.

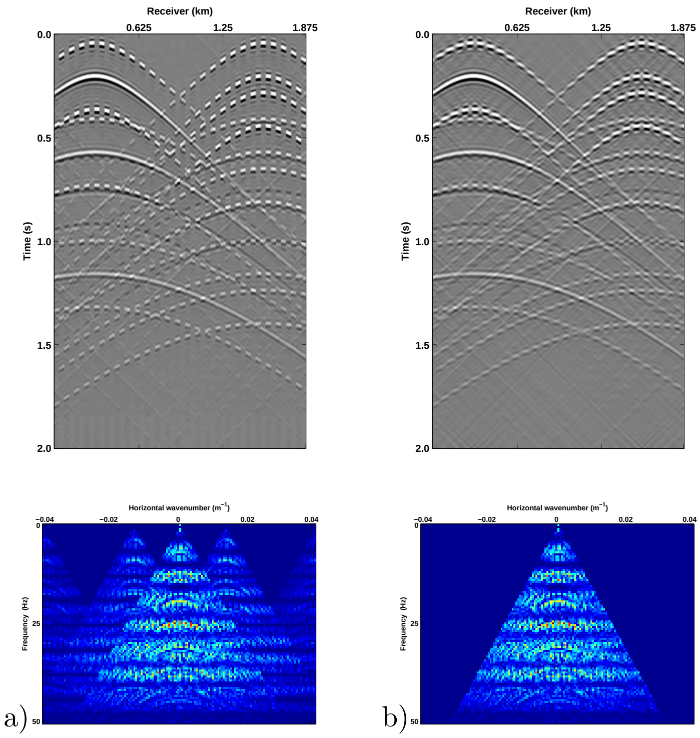

Figure 3-5: *Sampled shot gathers and their f-k spectra:* **(a)** *before f-k filter,* **(b)** *after f-k filter.*

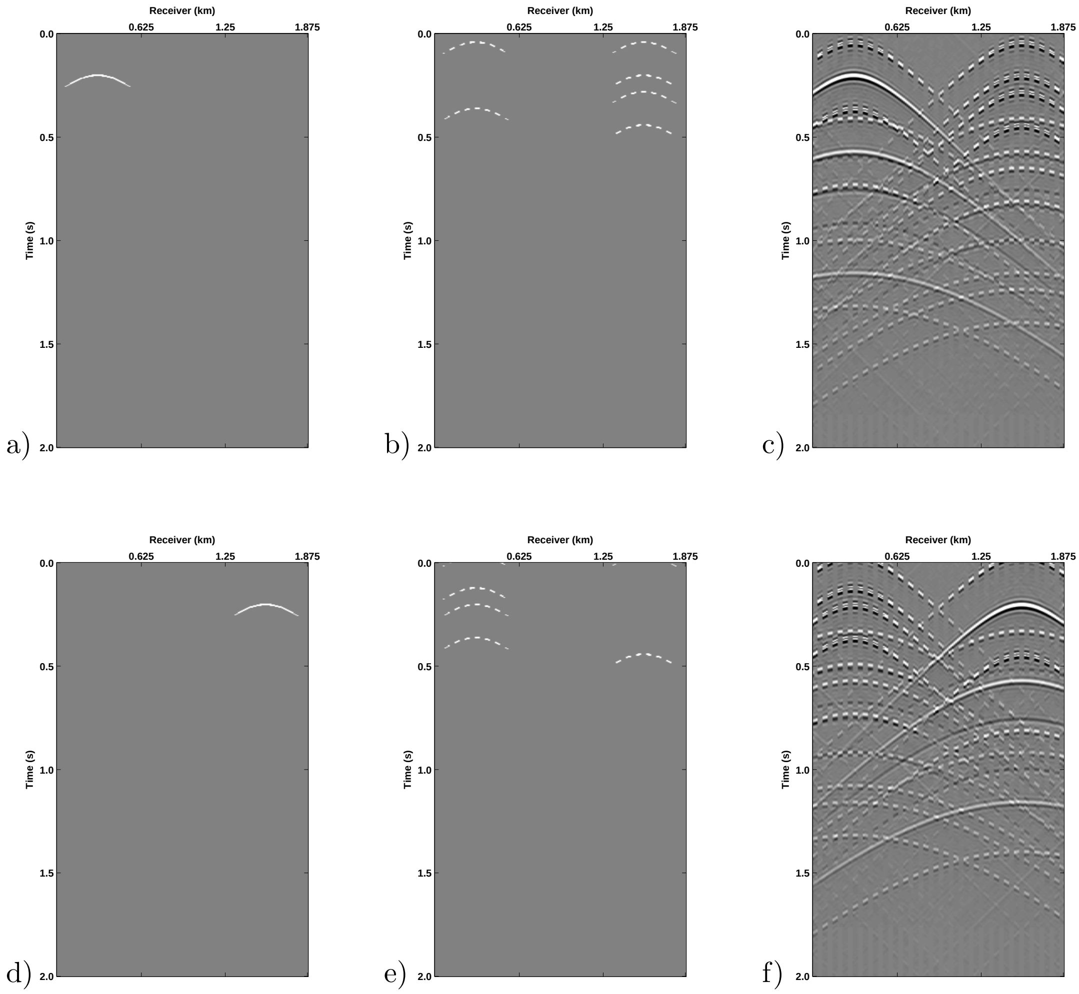

Figure 3-6: (**a** *and* **d**) *After threshold.* (**b** *and* **e**) *Estimated blending noise.* (**c** *and* **f**) *After subtracting the blending noise from the pseudo-deblended data.*

Noise estimation

The unblended estimates, $\bar{\mathbf{P}}_i$ (Figure 3-6 a and d), are used to predict the blending noise $\hat{\mathbf{N}}_i$ (Figure 3-6 b and e). The noise model can be formulated as:

$$\hat{\mathbf{N}}_i = (\,\bar{\mathbf{P}}_i \mathbf{\Gamma} \mathbf{\Gamma}_B^H\,)_{ss} - \bar{\mathbf{P}}_i. \tag{3-3}$$

Where "$(\,)_{ss}$" indicates the sample selection has been applied to the data between the brackets.

Note that, the estimated blending noise on the left in Figure 3-6 b and e, are related to the left source (Figure 3-6 a). The estimated blending noise on the right in Figure 3-6 b and e, are related to the right source (Figure 3-6 d).

Blending noise subtraction

The blending noise estimate, $\hat{\mathbf{N}}_i$, is subtracted from the pseudo-deblended and random-sample selected data. The results after subtraction are considered the deblending estimate, $\hat{\mathbf{P}}_i$ (Figure 3-6 c and f).

$$\hat{\mathbf{P}}_i = (\,\mathbf{P}_{sr} \mathbf{\Gamma}_B^H\,)_{ss} - \hat{\mathbf{N}}_i. \tag{3-4}$$

Iteration

The pseudo-deblended and random-sample selected data are used as the first deblending estimate in the iteration. Afterwards, the new generated deblending estimate, $\hat{\mathbf{P}}_i$, is updated at each iteration. The random-sample selection changes at each iteration, to reduce the chance of forming a coherent event in the blending noise.

Figure 3-7 shows the deblending estimate $\hat{\mathbf{P}}_i$ after certain number of iterations. Only deblending of the left shot is shown. The deblending of the right shot has the same behavior. A gradual removal of the blending noise in the shot gather is observed. Note that in this illustration, the random-sample selection is used. Comparing the deblended shot with the true shot in Figure 3-7 f, it is clear that deblending by shot repetition works well for synthetic data. Further discussion on the results is given in section 3-4.

3-2 Deblending by shot repetition with controlled sources

In this thesis, all the three types of configurations introduced in Chapter 1 are considered the shot-repetition acquisition with controlled sources. Because the delay time, position and the signature of all the blended sources are known. In the previous section, the type-II configuration is used to illustrate the deblending by shot repetition method. In this section, I will explain how to apply the same method to deblend type-I and type-III configuration data.

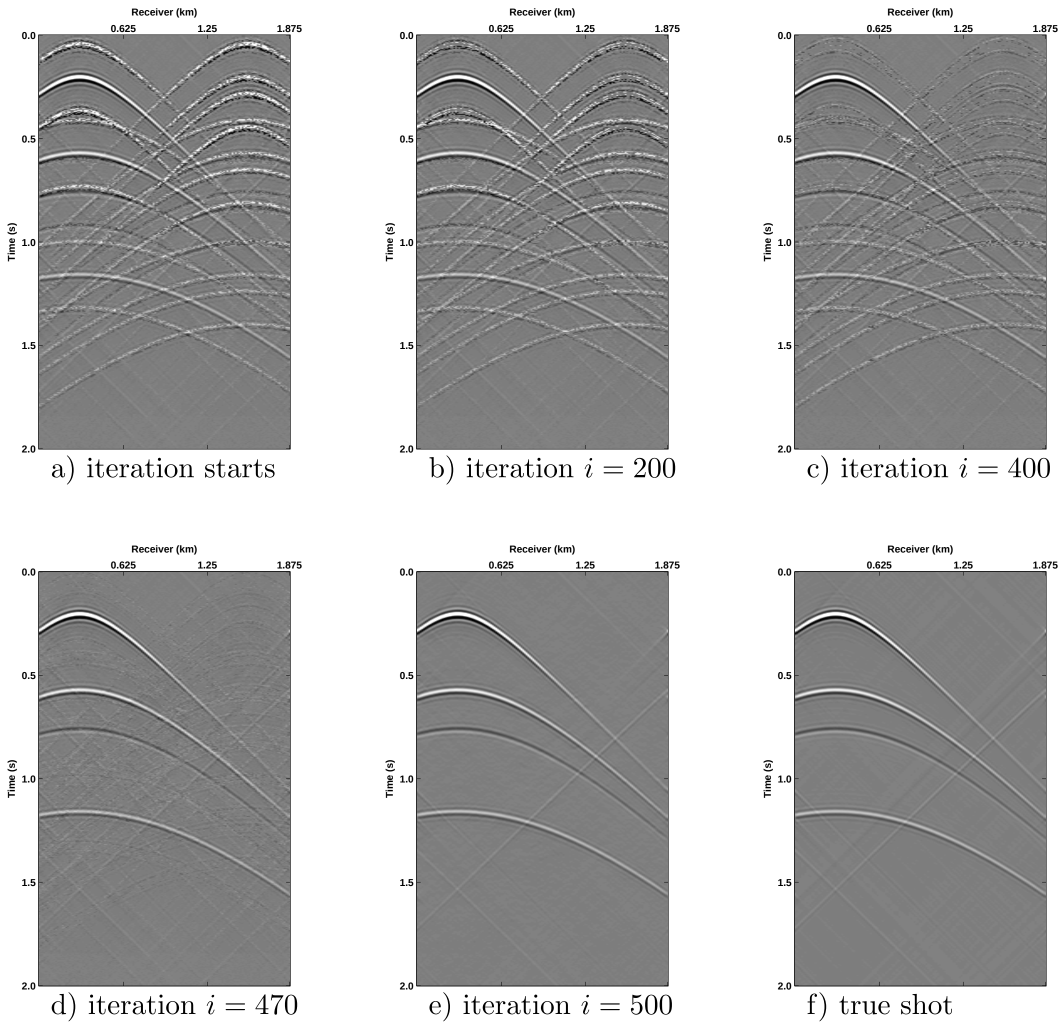

Figure 3-7: *The deblending estimate, $\hat{\boldsymbol{P}}_i$, at certain iterations.* **(a)** *A shot gather of the pseudo-deblended and random-sample selected data, i.e. the first deblending estimate.* **(b)** *after 200 iterations.* **(c)** *after 400 iterations.* **(d)** *after 470 iterations.* **(e)** *final deblended shot gather after 500 iterations.* **(f)** *The true unblended shot.*

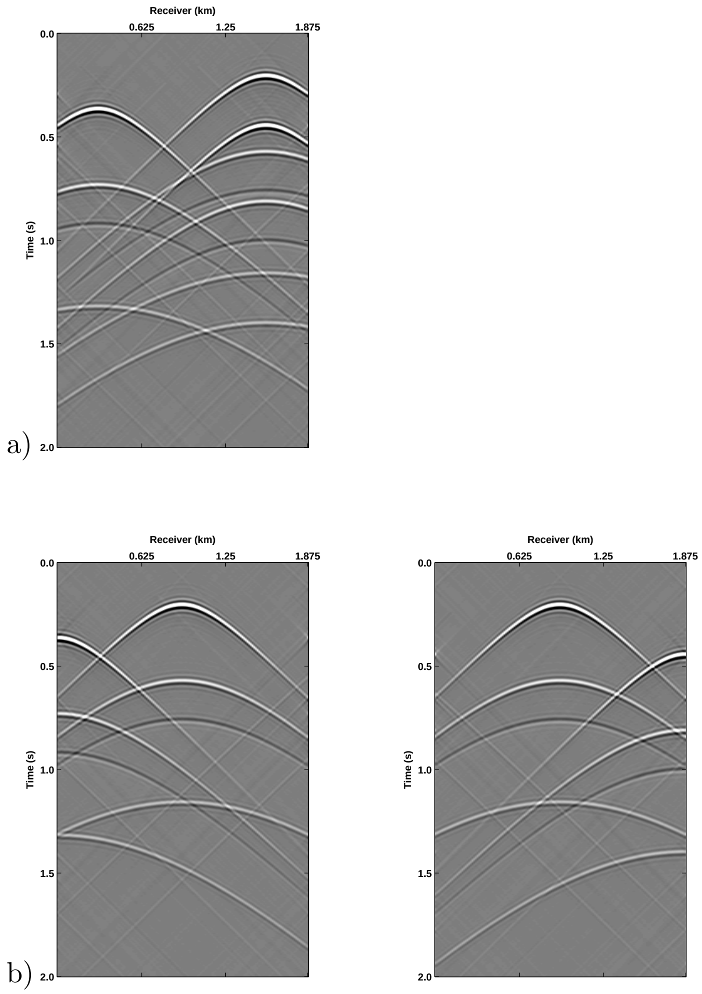

Figure 3-8: *Other configurations of shot repetition:* **(a)** *Type-I configuration,* **(b)** *Type-III configuration.*

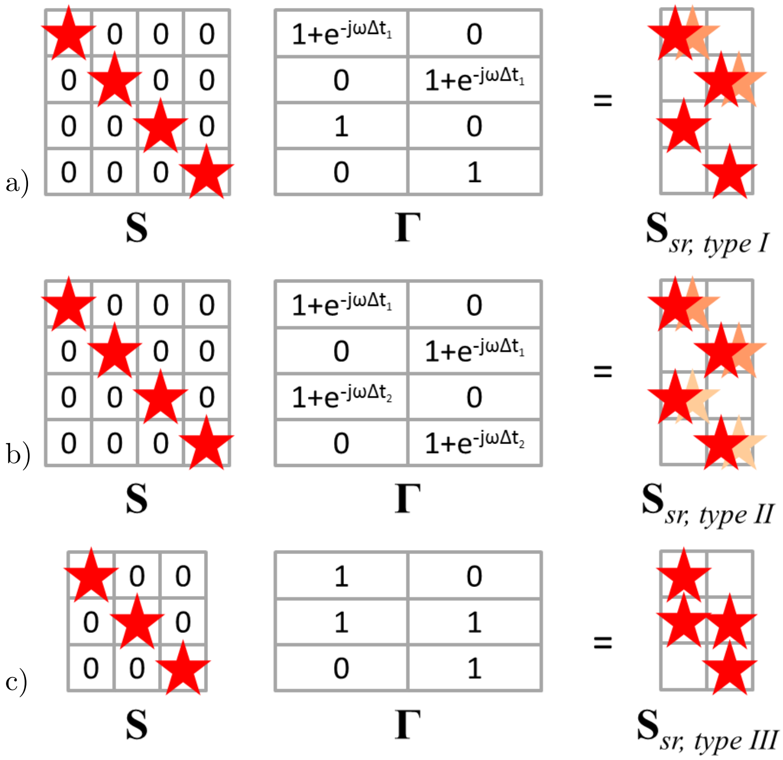

Figure 3-9: *Matrix operation in different types of shot repetition.* **(a)** *Type-I configuration,* **(b)** *Type-II configuration,* **(c)** *Type-III configuration.*

3-2-1 Type-I configuration deblending

For type-I configuration, there are three shots in one experiment. One shot is repeated while the other one is not (Figure 3-8 a). The blending matrix $\mathbf{\Gamma}$ of type-I is different from type-II. Figure 3-9 a illustrates the matrix operation of type-I shot-repetition blending. Non-zero elements of one column of $\mathbf{\Gamma}$ consists of a sum of two phase term in one element, $e^{-j\omega\Delta t_{kl,1}} + e^{-j\omega\Delta t_{kl,2}}$, and one phase term in one element, $e^{-j\omega\Delta t_{kl,1}}$.

The pseudo-deblending is only carried out for the repeating shots, due to the change of $\mathbf{\Gamma}$. Hence, after random-sample selection, only the repeating shots is coherent in the formed gather, and the incoherent events are considered the blending noise. The first threshold is designed for this coherent shot to select part of the unblended data after the *f-k* filter. It is called the first unblended estimate. The blending noise due to the repeated shot is estimated and is called the shot-repetition noise in this thesis.

To retrieve the non-repetitive shot, a second threshold is designed. The second threshold is applied after subtracting the first unblended estimate and the shot-repetition noise. The assumption is that the highest amplitude after subtraction of the first unblended estimate and the shot-repetition noise belongs to the non-repetitive shot. The second threshold is also lowered at each iteration.

The direct deblending result returns the repeated shot (Figure 3-10 a). The non-repetitive shot can be derived by using the known forward model and the delay time (Figure 3-10 b).

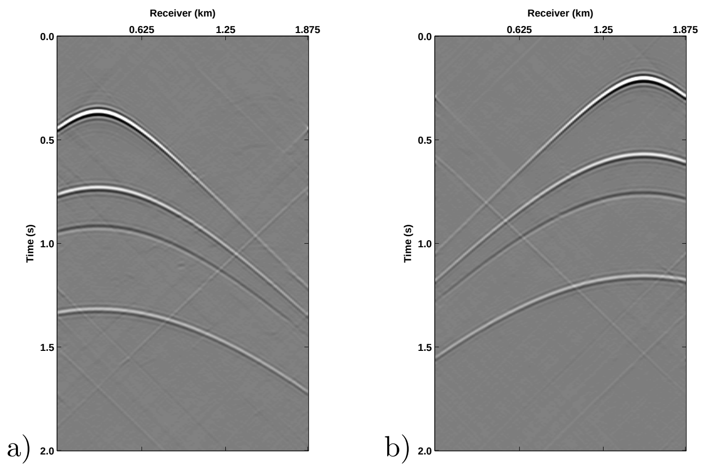

Figure 3-10: *type-I deblending results.* **(a)** *The deblended left shot,* **(b)** *the deblended right shot.*

3-2-2 Type-III configuration deblending

In type-I and type-II configuration, the deblending unit are both one shot gather. Different from those two, the deblending unit of type-III configuration consists of two experiments, i.e., two shot gathers. Each experiment contains two sources and one of the sources is repeated in the next experiment. An example is shown in Figure 3-8 b.

The deblending of type-III configuration requires two shot gathers. The pseudo-deblending removes the time delays of the repeating shots in both shot gathers, and random-sample selection forms new gathers. In the new gathers, only the repeating shots remain coherent, while the other two shots are incoherent. Similar as the type-I deblending, the first threshold only selects the unblended parts of the repeated shot. The second threshold is designed in the same way as the first threshold and it is based on the amplitude of the other two shots. The amplitudes of the non-repetitive shots are assumed to be the highest after subtraction of the first unblended estimate, i.e., the unblended part of the repeated shot, and the shot-repetition noise.

The direct deblending result returns the repeated shot (Figure 3-11 a). The non-repetitive shot can be derived by using the known forward model and the delay time (Figure 3-11 b and c).

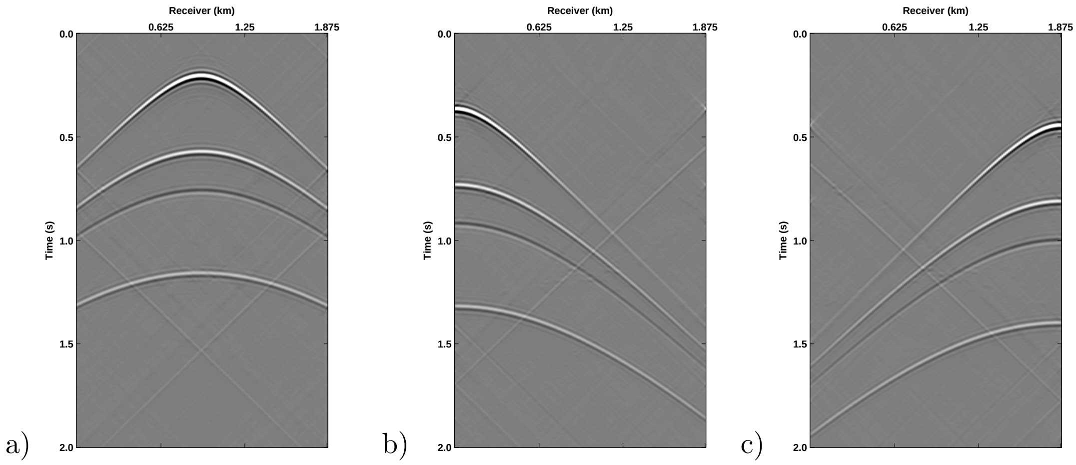

Figure 3-11: *Type-III deblending results:* **a)** *the repeated shot,* **b)** the left shot, ***c)*** the right shot.

3-3 Shot-repetition deblending with uncontrolled sources

In the presence of an uncontrolled wave field in the seismic data, the uncontrolled wave field can be seen as blending together with the seismic data. Usually, the uncontrolled wave field is considered noise and needs to be removed. The shot-repetition deblending with uncontrolled sources aims at removing the uncontrolled wave field. The following section introduce two special scenarios that falls in this category; deblending competitor's interference and deblending barnacle noise.

3-3-1 Competitor's interference

When a competitor's vessel is acquiring data in the neighbouring block, their signal is considered as noise to our data. It can be considered as a blending case without knowing the delay time of the competitor's source. Because the delay time is uncontrolled, the domain-switching deblending method cannot be applied in a straight-forward way. By shot repetition, however, it is possible to separate the competitor's interference form our own data. The scenario is similar to type-I configuration (Figure 3-8 a). The left non-repetitive shot is replaced by the interfering shot from a competitor ship in this case. The deblending result returns the desired shots, and the competitor's interference is considered as noise.

3-3-2 Barnacle noise

A barnacle is a type of marine shell animal that lives by attaching itself to eroded rocks or the bottom of a boat and feed in seawater. It turns out to be an issue when a large amount of barnacles attach themselves to the streamers. They cause strong interfering noise in the seismic data.

An example of barnacle noise is shown in Figure 4-5 a in Chapter 4.

3-4 Discussion on the synthetic data deblending results

The deblending results of synthetic data in three types are given in this chapter. In general, the algorithm performs well on separating interfering shots in the synthetic data.

In the type-I deblending results, the repeated shot is resolved well (Figure 3-10 b). The non-repetitive shot gather contains some imprint from the repeated shot (Figure 3-10 a). In the type-II deblending, two shots are repeated and in total four shots are blended in one gather. Both of the shots are resolved very well comparing with the unblended shots (Figure 3-7 e). In the type-III deblending, again the repeated shot (middle) is resolved well, while the other two shots containing signal leaked from the repeated shot (Figure 3-11). The results of three types are all near-perfect comparing with the unblended shot gathers. So there is no point pointing out which configuration is better here.

The algorithm operates solely in the shot gathers. Hence this method does not put restrictions on the source spacing. This also means that the algorithm can be easily extended parallel on a computer.

Chapter 4

Results on field data

In the previous chapter, examples of deblending by shot repetition on simple synthetic data are given, to illustrate the algorithm. Three types of shot repetition acquisition, and one specific scenario is discussed. In this chapter, I will demonstrate how this approach performs when applied to marine field data with the three configurations. I apply numerical blending to the conventionally acquired marine field data. The deblending results are compared with the unblended data.

4-1 Introduction

The marine field data was acquired using a conventional acquisition design by Petroleum Geo-Services (PGS) at the North Sea. The temporal and spacial sampling intervals are $4\,ms$ and $12.5\,m$, respectively.

The original seismic dataset is 3D. It is adjusted to a 2D split-spread dataset for easier processing. The preprocessing steps that have been applied were similar to what is described in Section 6.3 of van Groenestijn (2010). The preprocessed field data is blended numerically in different acquisition configurations.

I use the signal to noise ratio, SNR, to show the deblending error. The noise refers to the difference between the deblended data and the true data. It is calculated as follows:

$$SNR = 20\log_{10}\frac{rms\,(\,\mathbf{p}_{true}\,)}{rms\,(\,\mathbf{p}_{est}-\mathbf{p}_{true}\,)} \tag{4-1}$$

The function rms operates over all the elements of the input matrix. Every element of the input matrix is squared. The mean is computed over all the squared elements. The square root of the calculated mean is the scalar output of the function rms. $\mathbf{p}_{true}$ and $\mathbf{p}_{est}$ are the true data and the deblended data in space-time domain, respectively. Equation 4-1 provides a measure of the separability of the algorithm. In the measure of deblending results, the larger value of SNR shows that the deblended estimates have smaller error. When SNR is negative, it means that there is more blending noise than signal.

4-2 Results on deblending with controlled sources

4-2-1 Type-I configuration

The shot repetition data of the type-I configuration has been numerical blended from the 2D marine field dataset. A shot gather extracted from the blended data is given in Figure 4-1 a. The deblending results are given in Figure 4-1 b and c. Figure 4-1 d and e show the deblending error, i.e. the difference between the true shot gathers and the deblending results.

The strong early events from $0.0\,s$ to $1.2\,s$ are very well separated, especially considering they were strongly overlapping. The separation of weak events are less well resolved. This is because the strong events are sparser in the gather than the weak events. However, it is quite amazing that the weak flat reflections in the deep region ($2.0\,s$ to $3.0\,s$) are well delineated in Figure 4-1 c.

As discussed in Section 3-1, the data after pseudo-deblending and random-sample selection is the first unblended estimate. The SNR of the first estimate is $-0.85\,dB$, according to Equation 4-1. The SNR of the final deblending results is $6.0\,dB$. Hence, the enhancement in terms of the SNR, achieved by the algorithm is around $7\,dB$.

4-2-2 Type-II configuration

The shot-repetition data of the type-II configuration contains four shots in each shot gather. A shot gather extracted from the blended data is given in Figure 4-2 a. The deblending results are shown in Figure 4-2 b and c. Figure 4-2 d and e show the deblending error.

The strong early events from $0.0\,s$ to $1.2\,s$ are again very well separated. The events of low amplitude are not well resolved. However, it is quite amazing that the weak flat reflections in the deep region ($2.0\,s$ to $3.0\,s$) are well delineated in Figure 4-2 b and c.

The SNR of the first estimate in this configuration is $-3.1\,dB$, and the SNR of the final results is $8.5\,dB$. The deblending process achieved $11.6\,dB$.

4-2-3 Type-III configuration

In the shot-repetition data of type-III, two blended shot gathers are deblended to three individual shots. The blended gathers are shown in Figure 4-3 a and b. The deblended

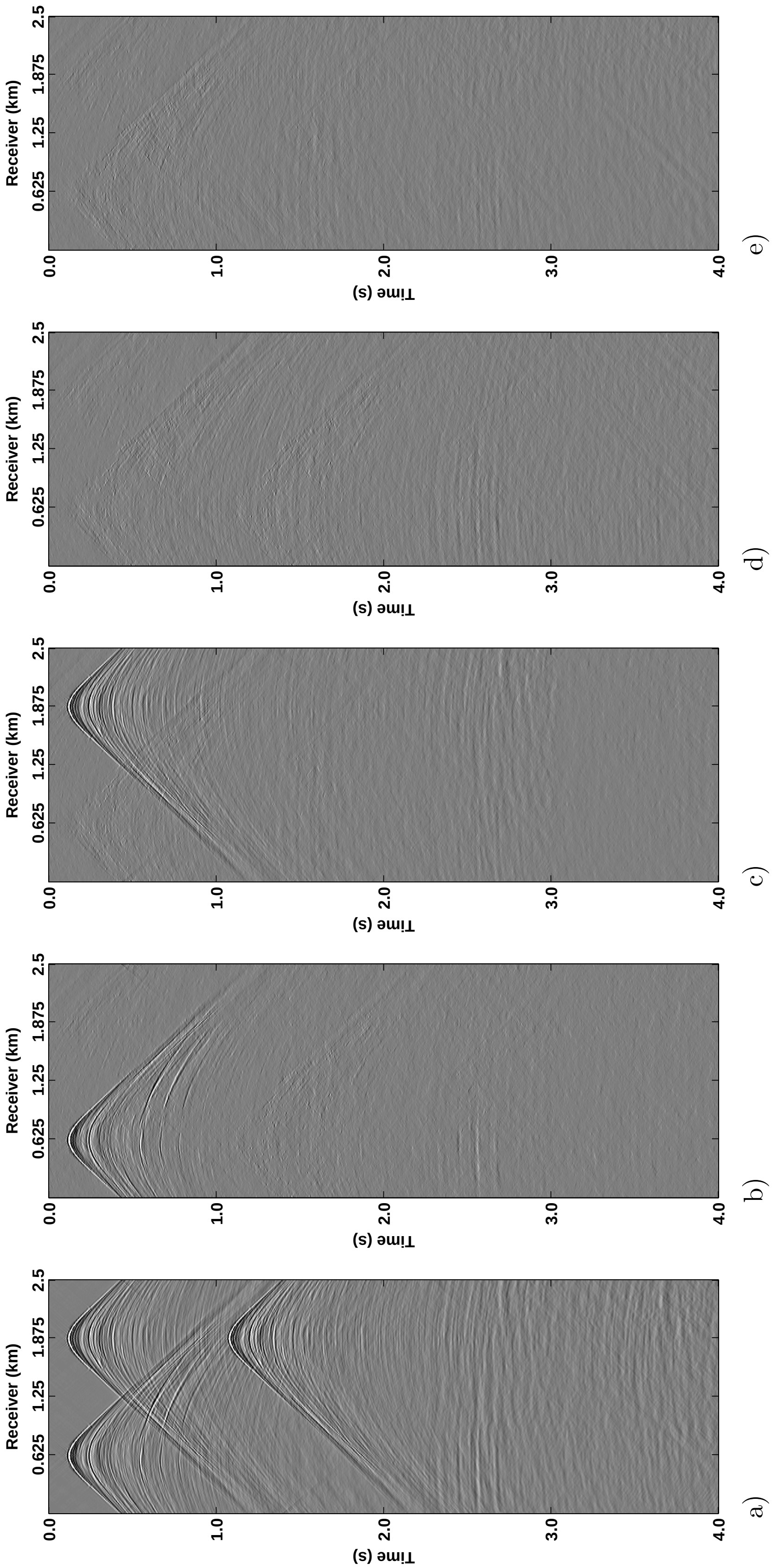

Figure 4-1: **(a)** *A shot gather of the type-I shot-repetition data.* **(b)** *The deblended shot gather (left shot).* **(c)** *The deblended shot gather (right shot).* **(d)** *The deblending error of the left shot.* **(e)** *The deblending error of the right shot.*

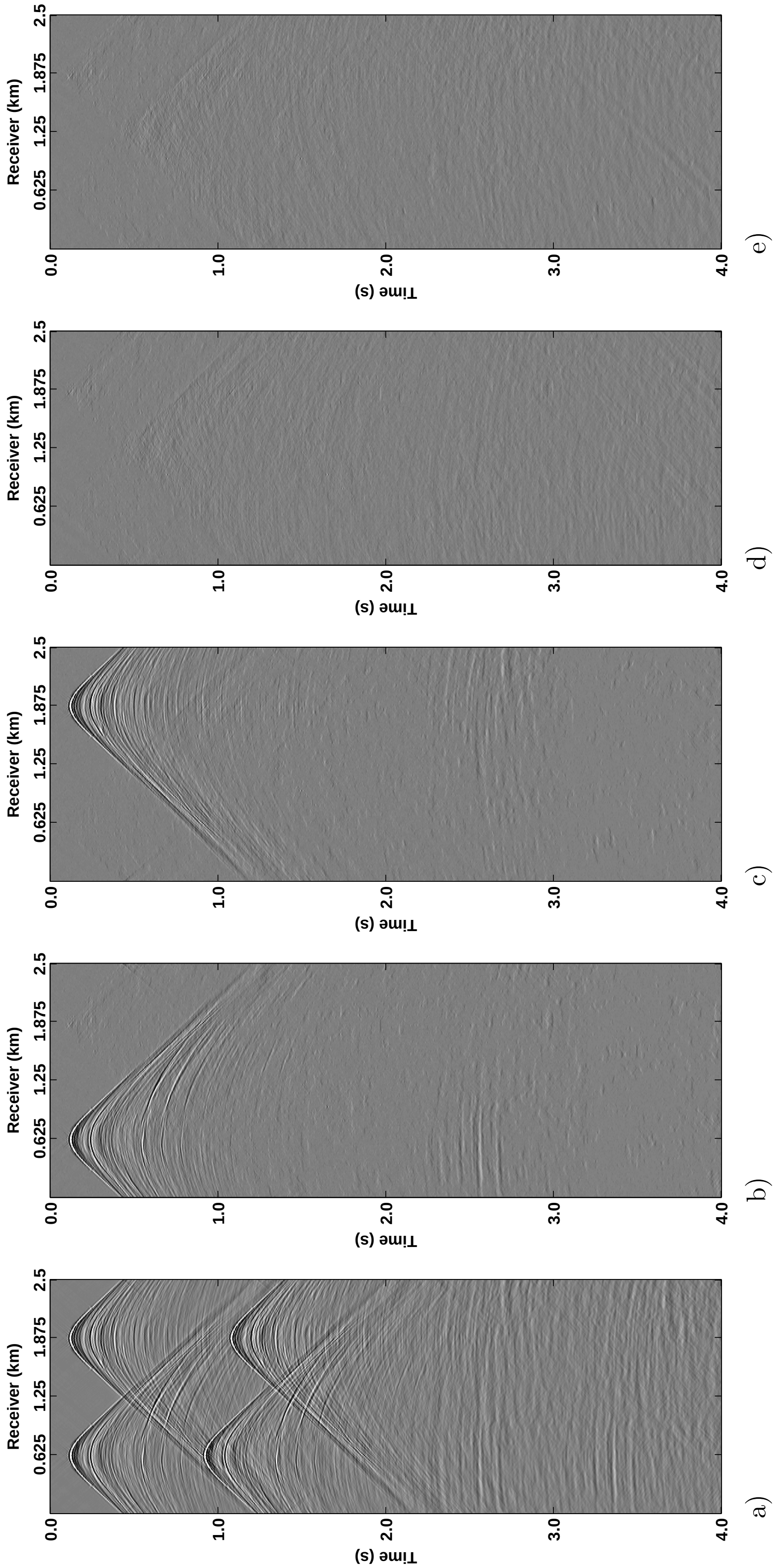

Figure 4-2: **(a)** *A shot gather of the blended data of Type 2 configuration.* **(b)** *The deblended shot gather of the left shot.* **(c)** *The deblended shot gather of the right shot.* **(d)** *The difference between the deblended shot gather and the unblended left shot.* **(e)** *The difference between the deblended shot gather and the unblended right shot.*

results are shown in Figure 4-3 c, d and e. Figure 4-4 shows the deblending error.

The strong early events from $0.0\,s$ to $1.2\,s$ are very well separated. The low amplitude events in general are not well resolved. The weak flat reflections located around $3.0\,s$ in Figure 4-3 c, d, e, are quite smoothly delineated. Comparing with the previous deblending results, the ability of resolving weak events in the type-III configuration is better. This is because where the weak events occurs ($1.2\,s$ to $2.0\,s$) are only two shots blended together. While in the type-I configuration, the problematic part is where three shots were blended, and in type-II configuration, it is where four shots were blended together.

The SNR of the first estimate is $0.3\,dB$, and the SNR of the final results is $7\,dB$. The deblending algorithm achieved $7\,dB$.

Chapter 3 shows the synthetic deblending results of three types. The SNR of the first estimates of the synthetic data all are around $-2\,dB$, and the SNR of the final results are around $20\,dB$. The deblending algorithm achieved approximately $22\,dB$ of SNR improvement on the synthetic data. In comparison with the SNR achievement of deblending synthetic data, the improvements of SNR in the field data example is fair.

4-3 Results on deblending with uncontrolled sources

4-3-1 Barnacle noise

Barnacle noise measured at the African west coast is scaled (Figure 4-5 c) and added to the numerically blended field data (Figure 4-5 a). The time delay between the repeating shots is $0.24\,s$. Deblending barnacle noise is similar with the type-I deblending, with the barnacle noise replacing the non-repetitive shot. Note that barnacle noise is not a real wave field. The deblended shot is shown in Figure 4-5 d and the deblended barnacle noise is shown in Figure 4-5 b.

Comparing with the unblended shot gather, Figure 4-5 d, the deblended shot shows that a big part of the barnacle noise is removed. There are high amplitude spikes left in the deblended shot that could not be removed by deblending. The SNR of the first estimate is $-2.1\,dB$, and the SNR of the final results is $2.6\,dB$. The improvement by SNR measure is $4.7\,dB$.

4-4 Discussion on the results

The above deblending results show that it is possible to deblend by shot repetition in a realistic setting. The deblending results depends on the types of overlapping events. In the deblended field data, the strong overlapping events can be separated quite well. When

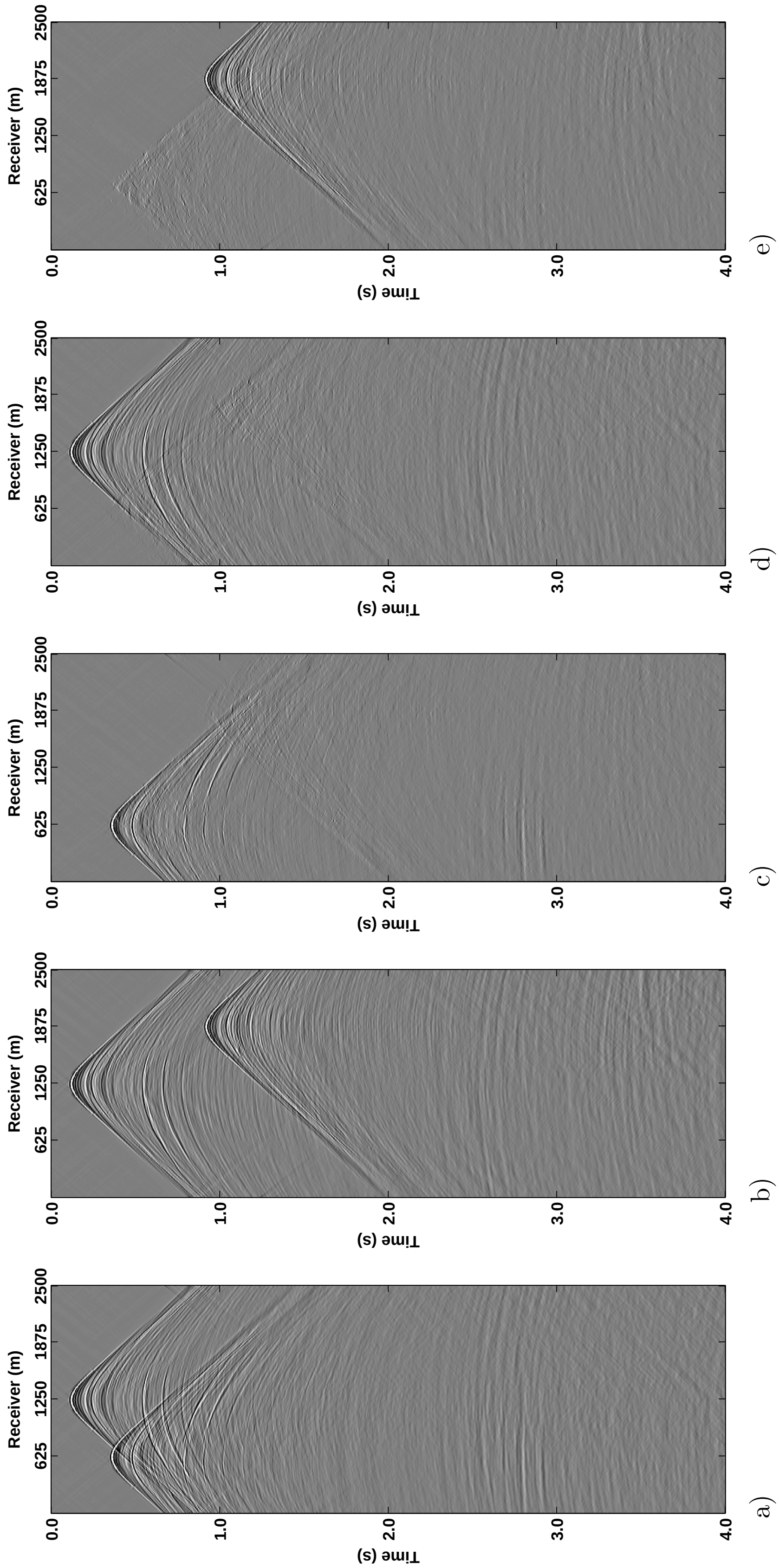

Figure 4-3: **(a)** *The first shot gather of the type-III shot-repetition data.* **(b)** *The second shot gather of the type-III shot-repetition data.* **(c)** *The deblended shot gather of the left shot.* **(d)** *The deblended shot gather of the middle shot.* **(e)** *The deblended shot gather of the right shot.*

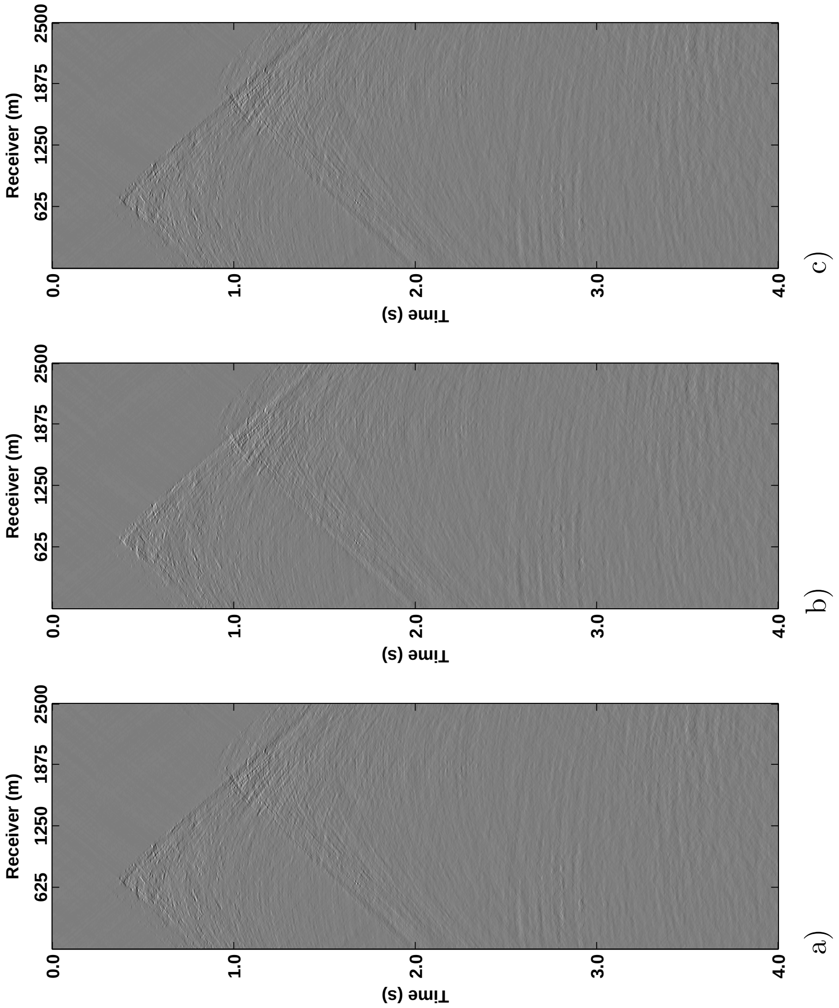

Figure 4-4: **(a)** *The deblending error of the unblended left shot.* **(b)** *The deblending error of the unblended middle shot.* **(c)** *The deblending error of the unblended right shot.*

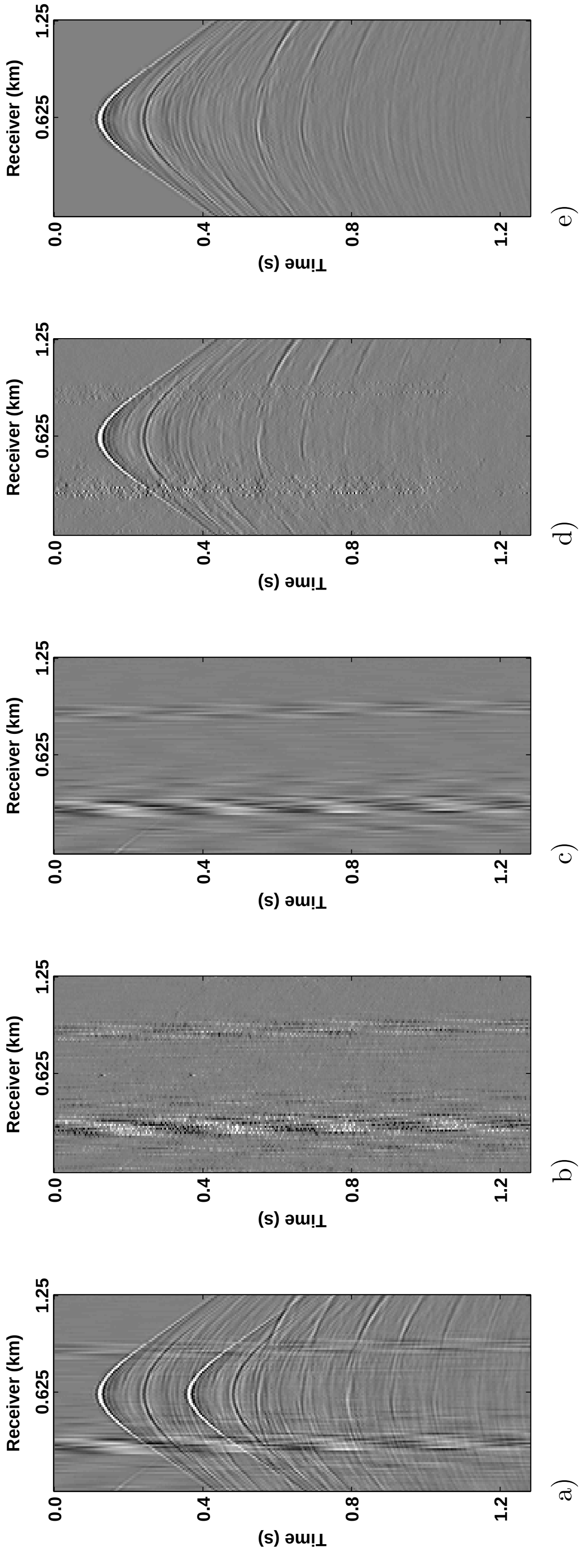

Figure 4-5: **(a)** *A shot gather of shot-repetition data contaminated with barnacle noise.* **(b)** *The deblended barnacle noise.* **(c)** *A shot gather of separated barnacle noise.* **(d)** *The deblended shot gather.* **(e)** *The unblended shot gather.*

weak events are overlapping with each other, the deblending results are not bad. This can be observed in the late flat events from around $2.0\,s$ to $3.0\,s$ in the deblended shot gathers. It is a good sign for practical concerns because the late events are quite often the most desired events. When weak events are overlapping with strong events, it is problematic. This can be observed especially in the region where one shot is interfering with the other shot's repetition. The energy from the weak events is leaked to the strong events and it causes blanks in the interfering regions. It is also observed in deblending barnacle noise, where parts of the strong barnacle noise cannot be removed. The algorithm has trouble identifying how much energy is coming from which shot.

In the algorithm, the coherency constraint is one of the major powers to deblend. In the method of Mahdad et al. (2011), the coherency constraint is applied after switching to another domain, where the desired signal is coherent and the blending noise is incoherent. I use the random-sample selection approach to allow applying a coherency constraint in the shot gather. But it could be that some parts of the interfering shots remain coherent after sample selection. Different random-sample selection at each iteration is used to reduce the chance of this to happen. However, if a part of the interfering noise remains coherent, it will be considered belonging to the aligned shot, and therefore causes error in the final deblending results. My current algorithm cannot solve this problem.

The coherency constraint is implemented as an *f-k* filter in this thesis. The *f-k* filter, however, is not a strong coherency pass filter because the incoherent energy that resides in the *f-k* signal cone, cannot be removed. The attenuation of this blending noise is aided by thresholding. One sample in the *x-t* domain is composed by various frequency components. Thus, with the help of the threshold, the incoherent energy gets more suppressed so that the coherent event stands out more.

However, thresholding causes signal leakage. When a weak event is crossing a strong event and the interference passes the threshold, the whole sample is contributed to the strong event and leave a blank in the weak event. A stronger coherency pass filter, and/or a better tool that selects the coherent events gradually, would improve the deblending results.

In the end, the results on the field data examples are very promising and there is still room for improvement on the algorithm's performance.

Chapter 5

Conclusions and discussions

5-1 Conclusions

Blended acquisition has become a hot topic because of its efficiency and data quality. Since the current industry processing standard cannot process the blended data directly, the blended data needs to be deblended as if they were acquired in the conventional way. Section 2-5 showed that the current deblending methods based on domain-switching are limited by sparse source sampling. This thesis has laid out a new acquisition design - shot repetition. It allows for deblending without the restriction on source sampling. The approach of deblending by shot repetition is tested and discussed, showing that it is promising to deblend by shot repetition.

The key elements of this approach are:

- Shot-repetition acquisition, as a type of blended acquisition, proposes to shoot more than one time at the same source location, to allow deblending soley in the shot gather.
- Deblending by shot repetition uses an estimation and subtraction of blending noise scheme, similar as the method of Mahdad et al. (2011). Instead of switching to another domain, I use random-sample selection to allow applying a coherency constraint in the shot gathers. Therefore, this method does not have any restrictions on source spacing.
- The major powers of deblending shot-repetition data are the coherency constraint and the sparsity of the seismic data. Shot-repetition data can be aligned in such a way that the interfering energy becomes incoherent. The coherency constraint is implemented in the *f-k* domain where an *f-k* filter attenuates the incoherent energy. Sparsity is implemented by a threshold in the *x-t* domain.
- Apart from deblending shot-repetition data with controlled sources, the algorithm can also be used for deblending uncontrolled sources, i.e. denoising. This thesis has discussed the application to data with competitor's interference and data with barnacle noise.

5-2 Discussion

Deblending is an underdetermined inverse problem, which has an infinite number of solutions. It is impossible to find a unique solution, but it is possible to find a solution that is closest to reality, by using the physical nature of seismic data. The data after pseudo-deblending and random-sample selection is one solution of the deblended data. Each shot gather of this data has a physical part, the desired coherent shots, and the unphysical part, the incoherent blending noise. The coherency pass filter removes (parts of) the incoherent energy.

I use an *f-k* filter as the implementation of the coherency constraint. However, this coherency pass filter is not sufficient enough. The interfering energy that mixed in the *f-k* signal cone cannot be removed. Therefore, I apply a threshold in the x-t domain to aid the coherency filter. The drawback of the current thresholding is that it causes signal leakage, because the threshold functions on a whole sample. A better tool that can select part of the coherent event iteratively is expected to work better than a simple threshold.

Practically, shot repetition would be valuable for 3D Marine seismic surveys, especially for wide-azimuth towed streamer acquisition. Usually, two sources are deployed and the streamer spread consists of several streamers at around $100\,m$ streamer separation. It would be helpful to have extra sources ahead of the conventional sources on the in-line direction to measure far offset, or place extra sources on the cross-line direction to measure different azimuths. The shot-repetition design allows more freedom on choosing source positions than the blended acquisition design of Vaage (2002).

It is possible to couple shot repetition with the existing equipment. Parkes and Hegna (2011) employ an equipment that fires two sources at the same location. Although they have made the two source signals deliberately different from each other.

5-3 Future plans

The deblending results on field data are promising. However, they also show that there is indeed room for the improvements discussed above. Another easy practical task would be suppressing the signal leaked above the water-bottom reflection, so that the leaked events are more likely to be assigned in the right place.

I hope to report on the improvements of the deblending by shot repetition algorithm during a two-month extension of my internship.

Bibliography

Beasley, C. J., Chambers, R. E., and Jiang, Z., 1998, A new look at simultaneous sources: SEG Technical Program Expanded Abstracts, **17**, no. 1, 133–135.

Berkhout, A. J., 1982, Seismic migration, imaging of acoustic energy by wave field extrapolation, a: theoretical aspects: Elsevier.

Berkhout, A. J., 2008, Changing the mindset in seismic acquisition: The Leading Edge, **27**, no. 7, 924–938.

Kontakis, A., and Verschuur, D. J., 2014, Deblending via sparsity-constrained inversion in the focal domain: 76th EAGE Meeting, Extended Abstract.

Mahdad, A., Doulgeris, P., and Blacquière, G., 2011, Separation of blended data by iterative estimation and subtraction of blending interference noise: Geophysics, **76**, no. 3, Q9–Q17.

Parkes, G., and Hegna, S., 2011, An acquisition system that extracts the earth response from seismic data: First Break, **29**, no. 12.

Peng, C., Liu, B., Khalil, A., and Poole, G., 2008, Deblending of simulated simultaneous sources using an iterative approach: An experiment with variable-depth streamer data:, *in* SEG Technical Program Expanded Abstracts 2013, 4278–4282.

Spitz, S., Hampson, G., and Pica, A., 2008, Simultaneous source separation: A prediction-subtraction approach:, *in* SEG Technical Program Expanded Abstracts 2008, 2811–2815.

Vaage, S. T., 2002, Method and system for acquiring marine seismic data by using multiple sources: US patent 6,906,981.

van Groenestijn, G. J. A., 2010, Estimation of primaries and multiples by sparse inversion: Ph.D. thesis, Delft University of Technology.

Womack, J., Cruz, J., Rigdon, H., and Hoover, G., 1990, Encoding techniques for multiple source point seismic data acquisition: Geophysics, **55**, no. 10, 1389–1396.

Acknowledgements

This thesis is carried out from March to August 2014, at PGS (Petroleum Geo-Services), Leiden in cooperation with TU Delft.

I want to thank all the people who have participated in this project, in particular my supervisor Dr. Ir. G.J.A van Groenestijn, for his support and guidance. Futhermore, I would like to thank Dr. Ir. G.G. Drijkoningen for the useful suggestions, Ir. R. Baardman and Dr. R. Hegge for reviewing my thesis, Dr. G. Blacquière for the inspiring talks, and all my colleagues at PGS Leiden: Dr. Ir. R. van Borselen, Dr. M. Frijlink, Dr. D. Könitz, and Dr. C. Riyanti, for their technical and spiritual support.

Delft University of Technology Sixue Wu

August 8, 2014